INORGANIC ELEMENTAL ANALYSIS OF WOODFORD AND MISSISSIPPIAN MUDROCKS: IMPLICATION FOR PETROLEUM SYSTEMS ANALYSIS

A Thesis

by

RYAN GARRETT WILCOXSON

Submitted to the Office of Graduate and Professional Studies of
Texas A&M University
in partial fulfillment of the requirements for the degree of

MASTER OF SCIENCE

Chair of Committee,	Franco Marcantonio
Committee Members,	Andrea Miceli Romero
	Michael King
Head of Department,	Mike Pope

May 2018

Major Subject: Geology

ABSTRACT

The Woodford Shale and the overlying Mississippian Limestone constitute one of the major oil and gas producing intervals across the Anadarko basin and adjacent shelves. Known for its organic-richness and generation potential, the Woodford Shale has long been recognized as a major source rock for produced oils from the Mississippian Limestone. However, variations in crude-oil composition, together with the presence of secondary organic-rich mudrocks within the Mississippian Limestone, provide another hydrocarbon charge source. Recent organic geochemical studies showed evidence for a contribution to the produced oils from Mississippian mudrocks, in addition to the Woodford Shale. Here, we use inorganic elemental analyses as an additional tool for unraveling source rock depositional settings and secondary processes associated with hydrocarbon generation and migration.

In this study, a collection of oil samples, together with core samples from Logan County in north-central Oklahoma, was examined using inductively-coupled plasma mass spectrometry (ICP-MS). Additionally, rock samples were analyzed using Rock-Eval for hydrocarbon generation potential assessment, and oil samples were processed for overall n-alkane profiles using GC-FID. Based on TOC and elemental composition signatures, samples from the organic-rich beds within the Mississippian section were divided into three intervals, and compared with the Woodford Shale samples. Average TOC values for organic-rich Mississippian rocks increase down section with an average of 5.8%, while TOC values for the Woodford Shale average 7.1%. The depth profile trend of major and trace elements such as Mg, Al, Fe, V, Ni etc. were compared with Rock-Eval and GC-FID data to evaluate organic matter type, preservation and redox condition, and hydrocarbon generation potential. Additionally, an inorganic elemental

fingerprint was developed for the rocks and compared with that of the crude-oil samples, with the aim to understand the use of elemental fingerprinting as a tool for oil-source correlation and/or secondary alteration processes as a function of hydrocarbon migration.

DEDICATION

This paper is dedicated to my amazing family. Without the love and support you all have provided me throughout the years, I would not be where I am today.

Thank you for everything.

ACKNOWLEDGEMENTS

I would like to thank my committee chair, Dr. Franco Marcantonio, and my committee members, Dr. Andrea Miceli-Romero and Dr. Michael King, for their guidance and support throughout the course of this research. I would also like to thank Ibrahim Al-Atwah and Dr. John Pantano for their ideas and guidance, Dr. Mauro Becker, Dr. Carlos Dengo and Dr. Mukul Bhatia for their support through the Berg-Hughes Center and the Chevron Center of Research Excellence Basin Modeling Program and Luz Romero for all of the guidance, support and long hours she dedicated to providing me with the best results possible.

I also give great thanks my wonderful parents, my family and my friends for all the love and encouragement they have provided me throughout my master's studies. I would not have been able to do this without them. I also give thanks to my colleagues and the Texas A&M University Geology and Geophysics department faculty and staff for making my time here a great experience.

CONTRIBUTORS AND FUNDING SOURCES

Contributors

This work was supervised by a thesis committee consisting of Dr. Marcantonio [advisor] and Dr. Miceli-Romero [member] of the Department of Geology and Geophysics and Dr. King [member] of the Department of Petroleum Engineering.

All work for the thesis was completed by the student, under the advisement of Dr. Marcantonio of the Department of Geology and Geophysics. Core and oil samples were provided by Ibrahim Al-Atwah and oil samples by the University of Oklahoma. The core and oil samples were analyzed on ICP-MS by Luz Romero. Organic analyses were performed by Aramco in Houston. All core and oil samples were digested and analyzed at Texas A&M University. Some oil samples were digested at GERG at Texas A&M University.

Funding Sources

Graduate study was supported in part by a fellowship from the Chevron Center of Research Excellence Basin Modeling Program of the Berg-Hughes Center and in part by an assistantship from the Berg-Hughes Center.

NOMENCLATURE

Al	Aluminum
Ca	Calcium
Co	Cobalt
Cr	Chromium
Cu	Copper
EF	Enrichment Factor
Fe	Iron
HF	Hydrofluoric Acid
HR-ICP-MS	High Resolution-Inductively Coupled Plasma-Mass Spectrometer
K	Potassium
Mg	Magnesium
Mn	Manganese
Mo	Molybdenum
Pb	Lead
Na	Sodium
Ni	Nickel
S	Sulfur
Ti	Titanium
TOC	Total Organic Carbon
TTM	Total Transition Metals
U	Uranium

V	Vanadium
Zn	Zinc

TABLE OF CONTENTS

Page

ABSTRACT ii

DEDICATION iv

ACKNOWLEDGEMENTS v

CONTRIBUTORS AND FUNDING SOURCES vi

NOMENCLATURE vii

TABLE OF CONTENTS ix

LIST OF FIGURES xii

LIST OF TABLES xv

CHAPTER I: INTRODUCTION 1

CHAPTER II: STUDY AREA AND GEOLOGICAL SETTINGS 3

2.1 Study Area 3
2.2 Regional Geology 4
2.2.1 The Anadarko Basin 6
2.2.2 The Anadarko Shelf 7
2.2.3 The Cherokee Platform 7
2.2.4 The Nemaha Uplift 8
2.2.5 The Woodford Shale 8
2.2.6 The Mississippian Limestone 10

CHAPTER III: METHODOLOGY 11

3.1 Sampling Interval 11
3.2 Inorganic Elemental Analysis of Core Samples 11
3.2.1 Pyrolysis Followed by Wet Digestion 12
3.2.2 Wet Digestion with No Pyrolysis 14
3.3 Inorganic Elemental Analysis of Oils 14
3.3.1 Wet Digestion of Whole Oil Samples 15
3.3.2 Wet Digestion of Asphaltene Portion 16
3.3.2a Fractionation of Whole Oil 16
3.3.2b Wet Digestion of Asphaltenes 17

CHAPTER IV: RESULTS 18

4.1 Core Samples 18
4.1.1 Inorganic Elemental Data 18
4.1.2 Organic Geochemical Data 18
4.2 Oil Samples 24

CHAPTER V: DISCUSSION 26

5.1 Trace Elements 26
5.2 Core Sample Analysis 27
5.2.1 Trace Element Ratios for Organic Matter Classification 27

5.2.2 Trace Element Ratios for Paleoredox Determination 32
5.2.3 Element EFs for Paleoredox and Depositional Environment Determination 35
5.2.3a U, V and Mo 37
5.2.3b Ni and Cu 40
5.2.3c Comparison of U, V and Mo with Ni and Cu 42
5.2.3d Covariation of Ni, Cu, Mo, U and V with TOC (wt. %) 45
5.3 Oil Sample Analysis 54
5.3.1 Organic Matter Classification in Oil Samples 55
5.3.2 Paleoredox Determination in Oil Samples 57
5.4 Classification and Correlation 57
5.4.1 Oil-Oil Correlations 58
5.4.2 Oil-Source Rock Correlations 59
5.5 Depositional Profile 62

CHAPTER VI: CONCLUSION 70

REFERENCES 72

APPENDIX A 81

LIST OF FIGURES

Page

Figure 1: Study area and sample locations adapted from Al Atwah et al. (2015) 3

Figure 2: Late Devonian (360 Ma) setting adapted from Blakey 9

Figure 3: Early Mississippian (345 Ma) setting adapted from Blakey 10

Figure 4: Stratigraphic column and measured depth (MD) for the studied interval 12

Figure 5: Laboratory workflow for inorganic analyses of core and oil samples 13

Figure 6: V vs. Ni for the Woodford Shale and the Mississippian Limestone core samples 28

Figure 7: V/Ni vs. Co/Ni for the Woodford Shale and the Mississippian Limestone core samples 29

Figure 8: Mo/Ni vs. Co/Ni for the Woodford Shale and the Mississippian Limestone core samples 30

Figure 9: Lewan (1984) diagram for all core samples in this study 33

Figure 10: Lewan (1984) diagram for core samples from the Woodford Shale 34

Figure 11: Lewan (1984) diagram for core samples from the Mississippian Limestone 35

Figure 12: U, V and Mo enrichment factors (EFs) for the Woodford Shale core samples 38

Figure 13: U, V and Mo enrichment factors (EFs) for the Mississippian Limestone core samples 39

Figure 14: Ni and Cu EFs for the Mississippian Limestone core samples 41

Figure 15: Ni and Cu EFs for the Woodford Shale core samples 41

Figure 16: New groups for the Woodford cores using U, V, Mo, Ni and Cu EFs 43

Figure 17: New groups for the Mississippian cores using U, V, Mo, Ni and Cu EFs 44

Figure 18: Diagram illustrating the relative enrichment of Ni, Cu, Mo, U and V vs. TOC, adapted from Tribovillard et al. (2006) 46

Figure 19: TOC wt.% vs. U EF for Woodford Shale core samples and Mississippian Limestone core samples 48

Figure 20: TOC wt.% vs. V EF for Woodford Shale core samples and Mississippian Limestone core samples 48

Figure 21: TOC wt.% vs. Mo EF for Woodford Shale core samples and Mississippian Limestone core samples 49

Figure 22: TOC wt.% vs. Ni EF for Woodford Shale core samples and Mississippian Limestone core samples 49

Figure 23: TOC wt.% vs. Cu EF for Woodford Shale core samples and Mississippian Limestone core samples 50

Figure 24: TOC wt.% vs. U EF for Mississippian Limestone core samples using the classification scheme from Tribovillard et al. (2006) 51

Figure 25: TOC wt.% vs. V EF for Mississippian Limestone core samples using the classification scheme from Tribovillard et al. (2006) 52

Figure 26: TOC wt.% vs. Mo EF for Mississippian Limestone core samples using the classification scheme from Tribovillard et al. (2006) 52

Figure 27: TOC wt.% vs. Ni EF for Mississippian Limestone core samples using the classification scheme from Tribovillard et al. (2006) 53

Figure 28: TOC wt.% vs. Cu EF for Mississippian Limestone core samples using the classification scheme from Tribovillard et al. (2006) 53

Figure 29: Ni vs. V for the oil samples 56

Figure 30: Co/Ni vs. V/Ni for the oil samples 56

Figure 31: V vs. Ni for Woodford Shale core samples, Mississippian Limestone core samples and the oil samples 61

Figure 32: V/Ni vs. Co/Ni for Woodford Shale core samples, Mississippian Limestone core samples and the oil samples 61

Figure 33: Depositional Profile for the Woodford Shale and Mississippian Limestone 64

Figure 34: Schematic model of the depositional profile for the Woodford Shale 68

Figure 35: Schematic model of the depositional profile for the Mississippian Limestone 69

LIST OF TABLES

Page

Table 1: Major and trace elements and total organic carbon (TOC) content for the core sample set 19

Table 2: Trace element ratios for the core sample set 21

Table 3: Major and trace element enrichment factors for the core sample set 22

Table 4: Major and trace elements for the oil sample set 24

Table 5: Trace element ratios for the oil sample set 25

Table 6: Redox classification of the depositional environments, after Tyson and Pearson (1991), reprinted from Tribovillard et al. (2006) 27

Table 7: Trace element concentrations for the core sample set using Rock Eval pyrolysis method 81

CHAPTER I

INTRODUCTION

Studies concerning the application of inorganic elemental analyses to shale resource plays have been increasing in number over the past couple of decades. Due to the rise in unconventional petroleum resources, the need for and development of new methods and approaches for better understanding source rock and reservoir petroleum characteristics, as well as paleodepositional environment indicators, have been in high demand. With the older, more common, and highly reliable methods and approaches only providing a portion of the data needed to build a full, accurate model, more innovative methods and approaches have begun to surface. One such approach, using inorganic geochemical analyses on known or potential source rocks and potentially corresponding oil samples, and integrating this data with organic geochemical analyses, has begun to expand and thrive in more recent years.

Geochemical analyses on source rocks and produced fluids is a major tool used in the exploration and production industry for source rock and reservoir petroleum characteristics and for paleodepositional environment indicators. While organic geochemical analysis is the more commonly-used method for studying such characteristics, inorganic analysis has proven to be a reliable method for determining important aspects of paleodepositional environment, which may allow for more accurate oil-source rock correlations and overall characterization of a given area. When integrated with organic geochemical analyses, the inorganic data can become a powerful tool for unraveling both source rock depositional settings and secondary processes associated with hydrocarbon generation and migration.

This thesis focuses on two major oil and gas generating and producing formations, the Woodford Shale and overlying Mississippian Limestone, that spread across the Anadarko basin and surrounding regions. High Resolution – Inductively Coupled Plasma – Mass Spectrometry (HR-ICP-MS) was used to measure the trace element concentrations of core samples, from the Woodford Shale and the Mississippian Limestone formations, and oil samples, produced from the Woodford Shale and the Mississippian Limestone reservoirs. Analyses of the determined trace element concentrations were completed with the end goals of determining the paleoredox conditions, depositional environments and organic matter type/source. Such an understanding is critical for correlating produced oils to the original source rocks, and diagnosing the relationships between inorganic trace element concentrations and organic geochemistry.

CHAPTER II

STUDY AREA AND GEOLOGICAL SETTINGS

2.1 Study Area

The study area of this project is located in the north west-north central regions of Oklahoma (Figure 1), including, specifically, Woods, Alfalfa, Lincoln, Logan, Blaine and Payne Counties. These regions of Oklahoma include the structural and depositional features of the Anadarko basin, the Anadarko shelf, the Cherokee platform and the Nemaha uplift. Blaine county lies within the Anadarko basin; Woods and Alfalfa counties lie within the Anadarko shelf; Lincoln, Logan and Payne counties are located within the Cherokee platform. The Nemaha uplift separates the Anadarko shelf from the Cherokee platform to the east. Core samples were taken from an area distal to the deep Anadarko basin and proximal to the Cherokee

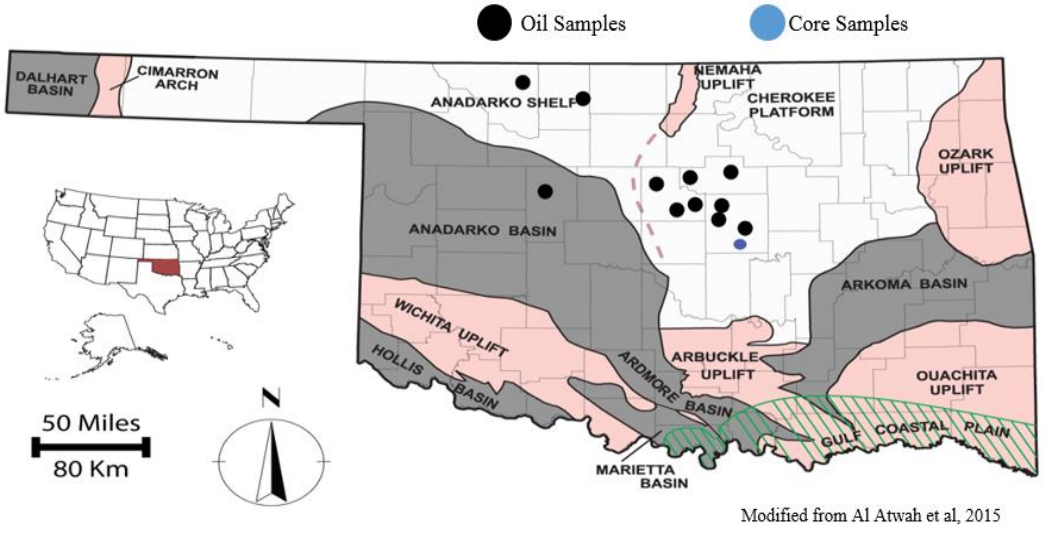

Figure 1: Study area and sample locations adapted from Al Atwah et al. (2015).

platform. The oil samples were taken from areas distal to the deep Anadarko basin and proximal to the Cherokee platform and Anadarko shelf.

2.2 Regional Geology

The present day geologic framework of Oklahoma and corresponding portions of the North American midcontinent has been, and continues to be, extensively researched. This area of the North American continent is composed of many major depositional and structural basins that contain great thicknesses of sediments and are situated atop a basement complex of Precambrian and Lower and Middle Cambrian igneous rocks and some low-rank metasedimentary rocks (Denison et al., 1984; Johnson et al., 1988; Northcutt et al., 2001). The basins throughout this region consist mainly of Paleozoic sedimentary rock of marine origin and are separated from one another by orogenic uplifts that were formed mainly during the Pennsylvanian time (Northcutt et al., 2001).

Northcutt et al. (2001) explain that, during the early Paleozoic, three major tectonic/depositional provinces existed in the region of present day Oklahoma. These three major provinces included the Oklahoma basin, the southern Oklahoma aulacogen, and the Ouachita trough. The Oklahoma basin, which, during the late Cambrian through the Mississippian time, was an embayment, or shelf-like area, that was covered by a broad epicontinental sea across most parts of the southern Midcontinent, received a remarkably thick sequence of shallow-marine carbonates interbedded with thinner marine shale and sandstones (Johnson et al., 1988; Johnson, 1989; Northcutt et al., 2001). The southern Oklahoma aulacogen, a west-northwest trending trough that included periods of crustal extension and faulting, was the depocenter for the Oklahoma basin and embraced a few of the many protobasins in the area including the Anadarko, the Ardmore and the Marietta (Cardott and Lambert, 1982; Northcutt et

al., 2001). The Ouachita trough was created by deep-water sedimentation along a rift at the southern margin of the North American craton (Northcutt et al., 2001).

Northcutt et al. (2001) explain that, throughout the middle Paleozoic, subsidence rates in the Oklahoma aulacogen slowed in Silurian and Devonian times and became much more rapid during Mississippian times. The Ouachita trough also experienced very large amounts of sedimentation throughout the Mississippian time. This sedimentation continued until the Pennsylvanian time, when the Oklahoma basin and the Oklahoma aulacogen were divided into a series of well-defined basins by sharply uplifted crustal blocks. The Ouachita trough was destroyed by these same uplifting events (Northcutt et al., 2001).

Klemme and Ulmishek (1991) explain that deposition of major source rocks occurred across the globe during the Silurian, Upper Devonian-Tournaisian, Pennsylvanian-Lower Permian, Upper Jurassic, Middle Cretaceous, and Oligocene-Miocene times. These source rocks have provided more than 90% of the world's discovered original reserves of oil and gas (Klemme and Ulmishek, 1991). Major petroleum-generating source rocks, throughout the area of study, include the Silurian marine shales of the Hunton Group, the Upper Devonian-Lower Mississippian Woodford Shale and the Pennsylvanian-Guadalupian basinal facies, marine shales.

Northcutt et al. (2001) explain that Silurian, Devonian, and Mississippian strata in Oklahoma comprise a moderately-thick to thick sequence of marine strata that underlie most parts of the state. This strata includes petroleum reservoirs that make up a significant portion of the overall petroleum production in Oklahoma. The major petroleum producing reservoirs, in the area of study, include the Silurian Hunton Group, the Upper Devonian Misener sandstone, the Upper Devonian-Lower Mississippian Woodford Shale, the Mississippian Limestone and the

Mississippian Chat. This study focuses on the Upper Devonian-Lower Mississippian Woodford Shale and the Mississippian Limestone.

2.2.1 The Anadarko Basin

The Anadarko basin, and its corresponding shelf, spans from the north Texas panhandle through western Oklahoma and into Kansas, where the Hugoton embayment begins. The Anadarko basin is the deepest sedimentary and structural basin in the cratonic interior of the United States (Johnson, 1989). The basin is bounded on the south by the Wichita and Amarillo uplifts, on the east by the Nemaha uplift, and on the west by the Cimarron arch (Johnson, 1989). This basin is known as being one of the greatest oil and gas provinces in the United States, and extensive exploration for hydrocarbons since the beginning of the 1900's has established a great amount of data for understanding the basin (Johnson, 1989).

Johnson (1989) explains that the history of the Anadarko basin can be divided into four major events including an igneous episode, an early epeirogenic episode, an orogenic episode, and a late epeirogenic episode. The igneous episode occurred during the Precambrian and early and middle Cambrian time and is described as the period when basement rocks were emplaced in the region currently known as the Anadarko basin. The early epeirogenic episode occurred from late Cambrian through Mississippian time and is described as the period when marine sediments were deposited in a broad epicontinental sea. The orogenic episode occurred during the Pennsylvanian time and is described as the period when the Oklahoma basin was broken into sharp uplifts and major basins. Structural activity during this period included folding, faulting, uplift and downwarping. The last episode, the late epeirogenic episode, began in the Permian time and is still persisting today. This period of time is described as including infilling of the

basin with Permian red beds, evaporates, and carbonates, and deposition of thin post-Permian strata uniformly across the basin and surrounding areas (Johnson, 1989).

2.2.2 The Anadarko Shelf

The northern shelf of the Anadarko basin extends across much of western Kansas, and part of it is referred to as the Hugoton embayment (Johnson, 1989). Koch et al. (2014) explains that, during the Mississippian, shallow-water carbonates were deposited on the northern part of the Anadarko Basin, known as the Anadarko or Burlington shelf. Multiple, previous studies have interpreted the Anadarko shelf as a carbonate-ramp environment (Lowe, 1975; Lane and DeKeyser, 1980; Gutschick and Sandberg, 1983; Watney et al., 2001; Franseen, 2006; Mazzullo et al., 2009; Koch et al., 2014) that covers much of present-day Kansas and Oklahoma (Witzke, 1990; Watney et al., 2001; Franseen, 2006; Koch et al., 2014). During the Mississippian, regional tectonic activity, associated with the Ouachita uplift, exposed the shelf and created an extensive unconformity that separates Mississippian from Pennsylvanian strata (Montgomery et al., 1998; Rogers, 2001; Watney et al., 2001; Watney et al., 2008; Mazzullo et al., 2009; Koch et al., 2014).

2.2.3 The Cherokee Platform

Hair (2012) explains that the Cherokee Platform extends south from southeastern Kansas and southwestern Missouri into central Oklahoma. The Cherokee platform is separated from the Anadarko Shelf to the west by the north-south trending Nemaha Uplift. The Cherokee Platform contains prolific petroleum source rocks and producing reservoirs which include the Woodford Shale and overlying Mississippian Limestone.

The region that the Cherokee Platform currently occupies was once the location of a vast stable shelf that was formed by the Arkoma basin and the Ouachita fold belt (Hair 2012). During

the Paleozoic, after the deposition of the Woodford Shale, the Marathon-Ouachita-Appalachian orogenic event was initiated by subduction of the proto-Atlantic Ocean, subsidence of the Arkoma shelf buried the Woodford Shale in the Ouachita trough, the Anadarko basin received maximum subsidence rates, and the Ardmore and Marietta basins also received high subsidence rates which, ultimately, created an isolation of the Cherokee Platform and Nemaha Uplift as structural highs in central Oklahoma (Donovan et al., 1938; Ziegler, 1989; Hair 2012).

2.2.4 The Nemaha Uplift

The Nemaha uplift, a major structural feature within the Midcontinent region, extends from southeastern Nebraska to central Oklahoma (Burchett et al., 1983). The uplift extends across Oklahoma, separating the Cherokee Platform from the Anadarko shelf and basin (Dolton and Finn, 1989) and the Arkoma basin from the Anadarko basin. Ultimately, it forms the eastern boundary of the Anadarko Basin. The uplift contains structural elements such as high-angle normal and reverse faults (Carlson, 1971; Cronenwett, 1956). The origin of the Nemaha uplift is believed to result from a narrow left-lateral strike-slip fault system during the Ordovician or possibly before (Amsden, 1975; McBee, 2003).

2.2.5 The Woodford Shale

The Woodford Shale is a highly prolific, organic-rich source rock that was deposited throughout the southern Mid-Continent region during the late Devonian and early Mississippian. This unit ranges in thickness from 200 to 900 ft. in the Anadarko Basin area and from 50 to 100 ft. in most of the shelf areas (Northcutt et al. 2001; Amsden, 1975). It is characterized as being a dark-grey to black fissile shale with high concentrations of marine organic matter.

The Woodford Shale was deposited during a time of sea level rise, on top of an unconformity that occurred following early Devonian sedimentation, uplift and erosion

(Northcutt et al., 2001). The basal member of the Woodford Shale, the Misener Sandstone, was deposited first and composed of weathered clastic debris from the uplifted and eroded, underlying units in the region. The shale members of the Woodford Shale group were deposited under anaerobic conditions during the rise of the Woodford-Chattanooga Sea across the midcontinent (Figure 2). Although most of the Woodford Shale is Late Devonian in age, Mississippian conodonts occur in the top few meters at several localities (Frezon and Jordan, 1979; Northcutt et al., 2001). Northcutt et al. (2001) explains that the base of the lowest Mississippian unit is commonly placed at the top of the Woodford Shale but that this boundary is more indicative of paleotectonic change than is the time-stratigraphic boundary within the upper part of the Woodford Shale (Frezon and Jordan, 1979; Northcutt et al., 2001).

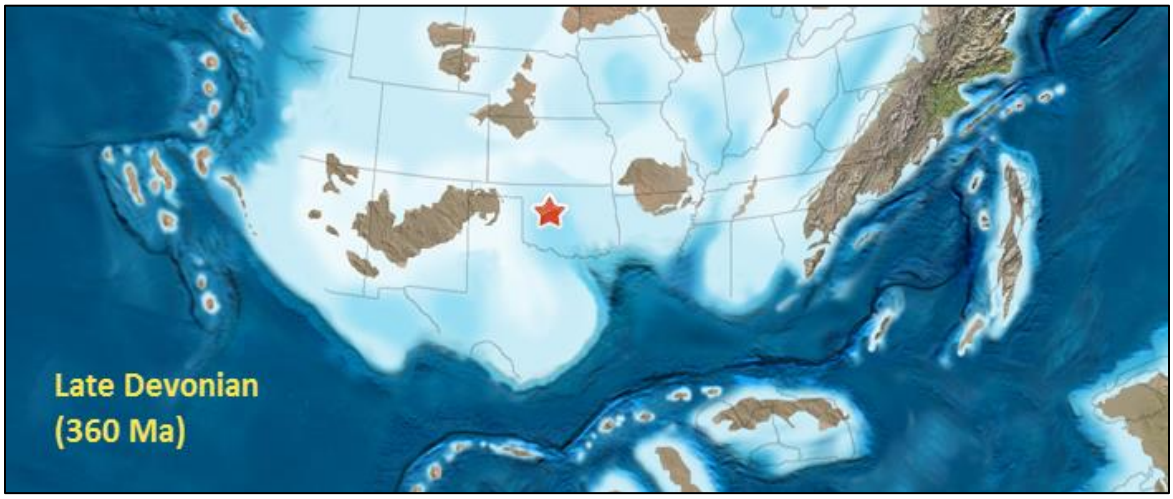

Figure 2: Late Devonian (360 Ma) setting adapted from Blakey (red star indicates study area).

2.2.6 The Mississippian Limestone

Mississippian carbonate rocks in northern Oklahoma and southern Kansas have been recognized, more recently, as prolific petroleum reservoirs (Boyd, 2012) and oil and gas fields producing from these reservoirs extend across large areas in Oklahoma and Kansas. Koch et al. (2014) explain that Mississippian deposits of Kinderhookian, Osagean and Meramecian age were deposited on top of Devonian deposits of the Woodford and Chattanooga Shales across the Anadarko shelf and basin (Montgomery et al., 1998; Rogers, 2001; Watney et al., 2001; Qi et al., 2007; Mazzullo et al., 2009).

After withdrawal of the euxinic seas, which deposited organic-rich black shales of the Woodford, the region was covered in Kinderhookian shallow, well-oxygenated marine waters. During Osagean time (Figure 3), the Osagean Sea developed across the continental interior, and sedimentation occurred in the southern Midcontinent. This sedimentation occurred in warm, shallow, oxygenated seas and limestone and cherty limestone were the dominant sediments. Northcutt et al. (2001) explains that a rich marine fauna, principally crinoids, flourished in this sea.

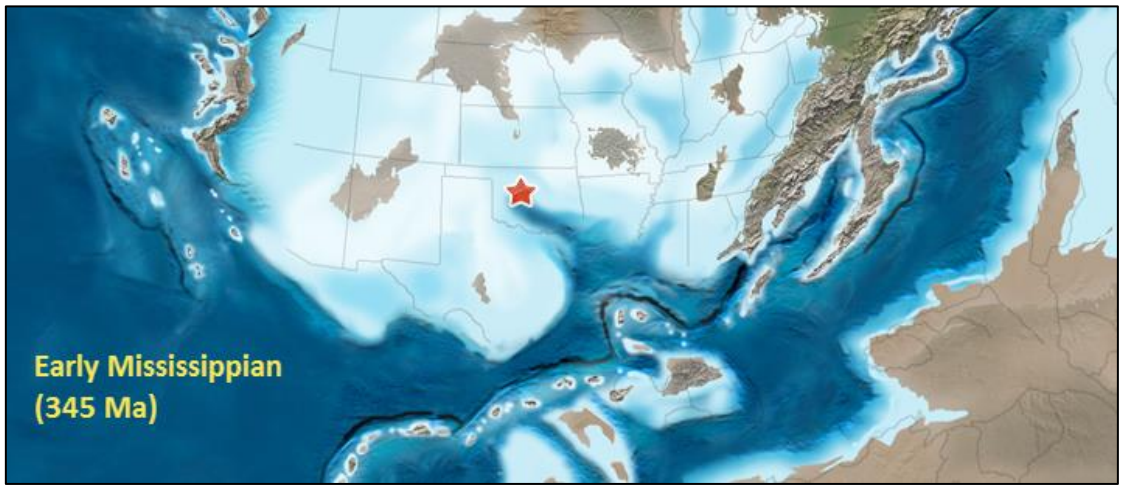

Figure 3: Early Mississippian (345 Ma) setting adapted from Blakey (red star indicates study area).

CHAPTER III

METHODOLOGY

3.1 Sampling Interval

A total of 36 core samples, from one well, and 11 oil samples, from 11 wells, were analyzed. Figure 1 shows the study area with the locations of the core and oil samples labeled in blue and black dots, respectively. Figure 4 shows a stratigraphic column representing the sampling interval from which the core samples were taken. Core samples were taken from fine-grained and dark-colored Mississippian and Woodford intervals from a well located in Lincoln County. Each core sample was pulverized, using a mortar and pestle, and stored in 15 mL centrifuge tubes. Oil samples were collected from Mississippian- and Woodford-producing reservoirs located in Woods, Alfalfa, Lincoln, Logan, Blaine and Payne Counties and were stored in glass beakers with Teflon screw caps. A workflow chart of the methods used in this study is shown in Figure 5.

3.2 Inorganic Elemental Analysis of Core Samples

Two digestion methods were performed on homogeneously pulverized core samples, 1) pyrolysis followed by wet digestion and 2) wet digestion with no prior pyrolyzation. Two sets of core samples, from the same intervals, were analyzed. One set of core samples was first sent to Saudi Aramco in Houston for Rock-Eval pyrolysis analysis and then analyzed at Texas A&M University Geology and Geophysics department for major and trace elements using an HR-ICP-MS. The second set of core samples were analyzed at Texas A&M University Geology and Geophysics department for major and trace elements using an HR-ICP-MS.

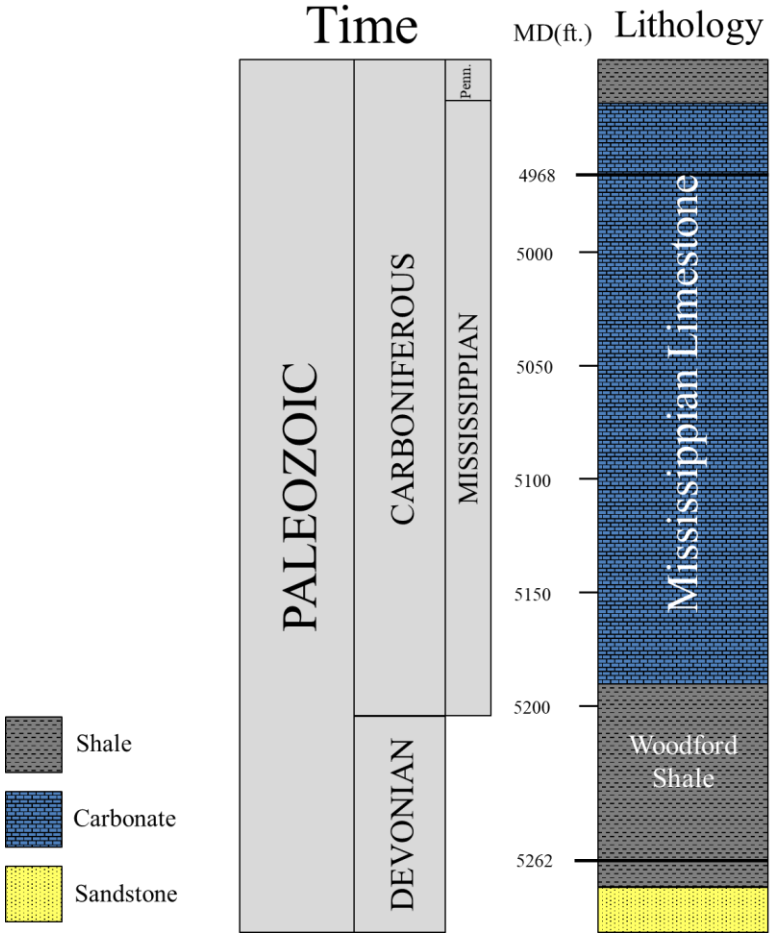

Figure 4: Stratigraphic column and measured depth (MD) for the studied interval

3.2.1 Pyrolysis Followed by Wet Digestion

For the pyrolysis method, approximately 60 mg of each pulverized core sample was weighed and sent to Saudi Aramco in Houston for Rock-Eval pyrolysis analysis. Rock powder residue was collected after undergoing combustion on the Rock-Eval instrument. The free-of-hydrocarbon, pyrolysized residue (inorganic components) was then returned to Texas A&M University Geology and Geophysics department and prepared for HR-ICP-MS analysis.

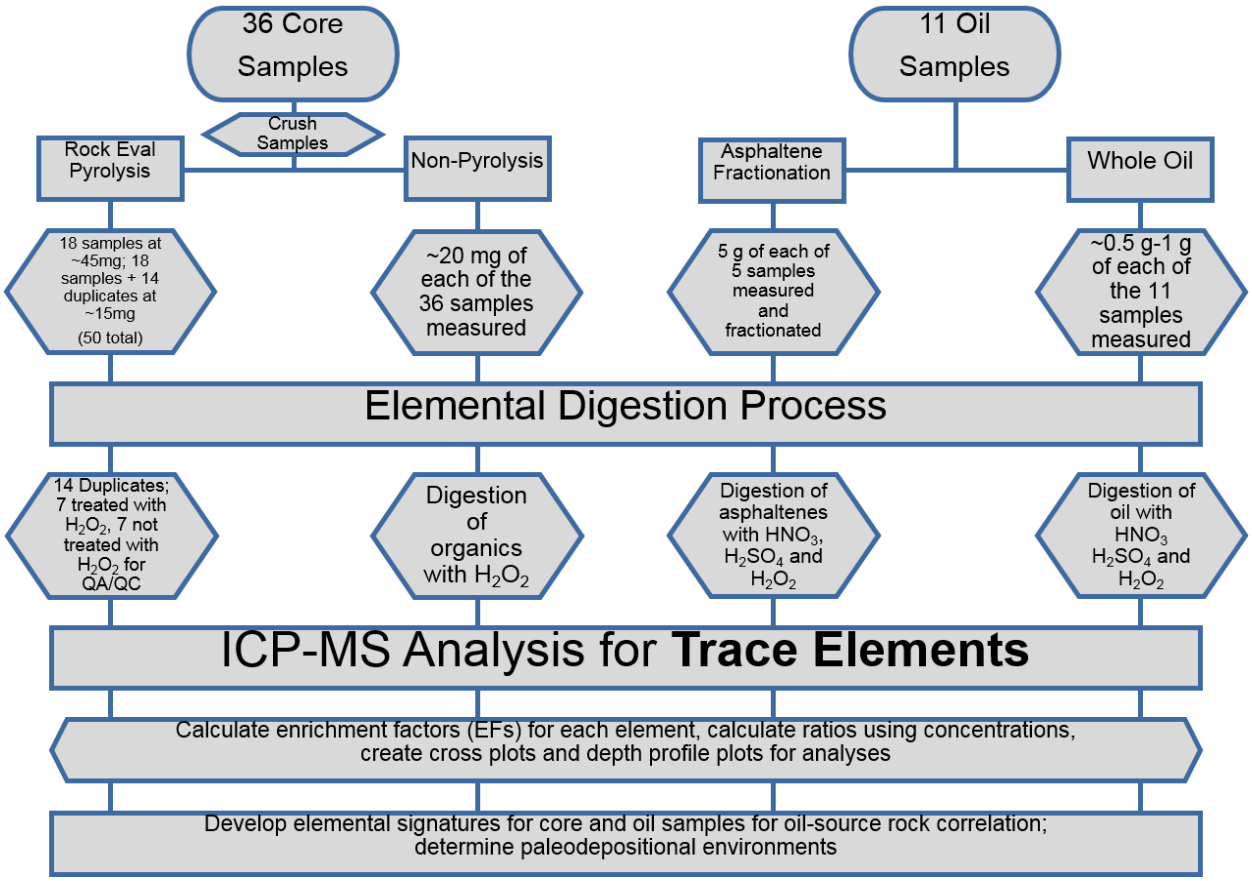

Figure 5: Laboratory workflow for inorganic analyses of core and oil samples.

Samples were numbered by depth, with sample 1 being the shallowest, and divided into 3 groups including: Group 1 (odd numbered samples) initial weights were ~45 mg, Group 2 (even numbered samples and 7 duplicates) initial weights were ~15 mg, and Group 3 which consisted of duplicates of 7, randomly chosen samples from group 2 and had initial weights of ~15 mg each. 3 Blanks and 3 standards were prepared and analyzed during the measurements of each of the 3 groups of samples. The standard used was an estuarine sediment sample from the National Institute for Standards and Technology (NIST 2702). A total of 50 rock samples were prepared. These 50 samples underwent a complete wet digestion using a cocktail of a combination of

ultrapure hydrofluoric (HF 48% m/m), perchloric ($HClO_4$ 72% m/m), and nitric (HNO_3 65% m/m) acids. The 7 duplicate samples from Group 2 underwent the exact same procedure as their originals, to check for consistency. The 7 duplicates from Group 3 were treated with 30% hydrogen peroxide (H_2O_2) to determine the presence of organics following the pyrolysis method. Upon complete digestion, the samples were diluted in ultrapure 2% HNO_3, and trace, minor and major elemental concentrations were measured by conventional HR-ICP-MS analysis.

3.2.2 Wet Digestion with No Pyrolysis

For the wet digestion method, approximately 20 mg of ground sample was placed in 15 mL Savillex breakers. Samples were paired with blanks and a standard (NIST 2702) for quality control, and digested in their respective heated Savillex (Teflon) beakers using a combination of ultrapure HF (48% m/m), $HClO_4$ (72% m/m), and HNO_3 (65% m/m). 30% H_2O_2 was used after the samples were removed from heat and cooled. H_2O_2 was used in case of the presence of undigested organic material. Upon complete digestion, the samples were diluted in ultrapure 2% HNO_3, and trace, minor and major elemental concentrations are measured by conventional HR-ICP-MS analysis.

3.3 Inorganic Elemental Analysis of Oils

A total of 11 oil samples were collected from wells producing from Mississippian and Woodford reservoirs in Woods, Alfalfa, Lincoln, Logan, Blaine and Payne Counties. The samples were stored in glass containers with Teflon screw-on caps. Two methods of digestion and analysis were performed on the oil samples, prior to measurement on HR-ICP-MS, to determine the most reliable and efficient method of elemental analysis. The methods include: 1) wet digestion of whole oil samples and 2) fractionation of the whole oil samples followed by wet digestion of the asphaltene portion.

3.3.1 Wet Digestion of Whole Oil Samples

For the wet digestion of 11 whole oil samples, approximately 0.25 g of whole oil was weighed and transferred to 15 mL Savillex (Teflon) beakers with screw-on caps. The samples were paired with a blank and a standard (NIST 1634c). Ultrapure sulfuric acid (H_2SO_4) was added to each sample in order to breakdown the oil phase. The samples were then covered tightly with the screw-on caps and placed on the hot plate at 120ºC for approximately one day. This use of H_2SO_4 and the screw-on caps allowed for a slight pressure build-up, aiding in the overall breakdown of the oil phase. The built-up pressure was released upon removal of the caps, in order to add 16M HNO_3 to each sample. Addition of HNO_3, followed by reflux, occurred 4 times throughout the period of approximately one day. Uncovering of the samples to allow for evaporation occurred when needed, for short periods of time, as to avoid as much exposure to contaminants as possible.

Once the samples were evaporated down, they were removed from the heat and cooled to room temperature. 30% H_2O_2 was then added to each sample for the digestion of organic compounds. For the addition of H_2O_2, samples needed to be at room temperature when using small volume beakers due to the vigorous reaction that occurred when the samples were heated. Once the samples completed their vigorous reactions with H_2O_2, they were set back on the hot plate and covered for reflux or, if necessary, left uncovered for evaporation. The addition of H_2O_2, to the samples at room temperature, followed by reflux or evaporation, occurred as needed throughout the span of approximately one day.

Due to time constraints, the samples were transferred (using HNO_3 to rinse the 15 mL beakers) to 150 mL or 200 mL Teflon beakers, covered with convex plates, in order to increase the surface area (heat exposure to samples), volume capacity (allowing addition of higher

volume of acids) and height of the beaker walls (decreasing the chance of overflow due to vigorous reactions with H_2O_2). Once transferred, higher volumes of H_2O_2 and HNO_3 (up to 4 mL of each) were added, in multiple stages, to the samples at greater temperatures (up to 170ºC). These modifications in the procedure greatly reduced the digestion time.

Upon complete digestion of the samples, a foggy-clear solution was present. After evaporating as much of the solution as possible, 1 mL of each sample solution was taken and weighed into 50 mL centrifuge tubes. 500 microliters of 100 ppm Indium (internal standard to monitor for machine drift) was added and the centrifuge tubes were then filled to 50 mL with 2% HNO_3. Trace, minor and major elemental concentrations are measured by conventional HR-ICP-MS analysis.

3.3.2 Wet Digestion of Asphaltene Portion

3.3.2a Fractionation of Whole Oil

For the wet digestion of the asphaltene portion, fractionation of the whole oil samples had to be performed first. This fractionation procedure was performed at the Geochemical and Environmental Research Group (GERG) at Texas A&M University. Of the 11 oil samples, only 5 of the samples were fractionated due to the quantity of the samples.

Approximately 5 g of whole oil sample was weighed into glass vials and filled to the top with pentane (C_5H_{12}). C_5H_{12} was used for this method due to its ability to precipitate asphaltenes out of solution. After allowing the asphaltenes to precipitate completely, the samples were transferred into flat bottom, glass boiling flasks, through a funnel and filter used to catch the asphaltenes. The glass vials were then rinsed using C_5H_{12}. Once the C_5H_{12} had completely passed through the filter, the funnel and filter were transferred to separate flat bottom, glass boiling flasks and rinsed with dichloromethane (CH_2Cl_{12}). CH_2Cl_{12} was used in this step due to

its ability to completely dissolve asphaltenes. This allowed the asphaltenes to completely pass through the filter and be transferred to the boiling flasks. Upon completion of transferring the asphaltenes, the boiling flasks containing the asphaltenes were placed in a hot water bath and set to 65ºC, to allow for the evaporation of the CH_2Cl_{12}. Once the CH_2Cl_{12} was evaporated, the remaining solution was transferred, using glass pipets, into 15 mL Savillex (Teflon) beakers and transported to the Texas A&M University Geology and Geophysics department for digestion of the asphaltenes and analysis on the HR-ICP-MS.

3.3.2b Wet Digestion of Asphaltenes

The asphaltenes were weighed into new 15 mL Savillex (Teflon) beakers with screw-on caps. Each of the asphaltene samples were of different weights which depended on the heaviness of each oil sample. The heavier oils, determined by visual thickness and viscosity, had a larger percentage of asphaltenes because the asphaltenes make up the heaviest portion of the oils. The wet digestion of asphaltenes procedure followed exactly the procedure stated in section *3.3.1 Wet Digestion of Whole Oil Samples*.

CHAPTER IV

RESULTS

The results from the HR-ICP-MS analyses of the core and oil samples are shown in the tables below (Tables 1-5). The initial analyses were run on 36 core samples and 11 whole oil samples. Organic geochemical data was obtained through use of Rock-Eval pyrolysis, as discussed in section *3.2.1 Pyrolysis followed by wet digestion* on the core samples.

After reviewing the results obtained, 3 of the core samples were not used because of inaccurate results due to either a possible misplacement of the samples in the studied interval, with respect to depth, or to altered results of trace elements during sample processing. Therefore, a total of 33 core samples and 11 whole oil samples are discussed in this study.

4.1 Core Samples

4.1.1 Inorganic Elemental Data

Tables 1, 2 and 3 show the inorganic elemental concentrations, the trace element ratios and the trace element enrichment factors, respectively, for the core samples in this study. The previous mentioned pyrolyzed core samples were not used in this study due to a possible contamination of Mo and Ni during the Rock-Eval procedure.

4.1.2 Organic Geochemical Data

Total organic carbon (TOC) content of the core samples is shown in Table 1. Within the 33 core samples, TOC contents range from 0.5 to 9.4 wt.% with an average of 3.9 wt.%. Woodford Shale TOC contents range from 2.1 to 9.4 wt.% with an average of 6.9 wt.%. Mississippian Limestone TOC contents range from 0.5 to 9.1 wt.% with an average of 3.2 wt.%.

Table 1: Major and trace elements and total organic carbon (TOC) content for the core sample set (n.d. means not determined).

Interval	Sample	Depth	TOC	Ti	Mn	Ni	Cu	Pb	U	Co	Mo
		ft.	wt. %	ppm	ppm	ppm	ppm	ppm	ppm	ppm	ppm
Mississippian Limestone	1	4,968.5	2.2	2,385	250.6	52.7	25.5	27.6	3.6	6.6	4.1
	2	4,972	2.1	3,765	154.2	55.7	27.1	21.4	3.5	10.3	7.2
	3	4,973	1.7	3,315	223.8	53.5	24.9	22.7	3.5	10.8	6.8
	4	4,975	4.0	2,391	185.6	70.7	31.4	20.6	4.1	6.9	9.6
	5	4,983	9.1	3,087	161.8	136.1	45.2	14.0	14.5	10.0	18.4
	6	4,992	4.4	3,132	177.7	115.6	36.2	19.1	17.2	10.4	24.1
	7	5,022	1.8	3,144	118.4	29.3	17.1	9.9	3.5	5.7	1.6
	8	5,033	2.7	2,763	283.2	74.0	22.4	14.0	11.5	10.3	12.9
	9	5,044	4.0	2,217	185.9	65.5	22.9	13.9	10.8	8.9	12.4
	10	5,050	6.9	3,097	123.2	172.8	58.5	19.1	18.3	11.5	23.0
	11	5,055	2.7	3,478	151.4	71.7	30.2	16.5	8.1	12.8	8.5
	12	5,059	2.8	4,259	119.0	66.6	32.2	17.6	7.9	13.9	9.3
	13	5,075	5.0	2,345	128.3	130.8	35.4	14.4	18.2	10.7	13.5
	14	5,086	1.8	3,462	149.7	52.3	22.0	15.7	5.6	10.9	4.1
	15	5,091	1.9	3,614	136.6	53.7	30.9	14.4	5.8	11.8	4.3
	16	5,099	1.3	2,785	201.1	41.5	19.4	12.8	4.3	10.8	3.4
	17	5,108	2.2	2,882	171.5	45.5	20.2	14.1	5.8	9.8	3.7
	18	5,112	3.6	2,930	153.3	80.3	26.3	15.1	9.3	12.3	8.1
	19	5,117	2.4	3,768	132.1	53.3	38.7	14.9	4.2	11.3	1.4
	20	5,120	3.1	4,034	123.1	84.9	45.6	15.5	5.9	12.4	4.1
	21	5,147	0.5	2,601	232.1	14.7	11.7	11.9	3.0	6.7	0.8
	22	5,150	0.6	2,113	326.3	28.7	14.5	8.3	2.9	6.8	0.7
	23	5,156	4.4	3,875	155.9	81.8	43.5	17.7	5.6	14.6	3.9
	24	5,160	2.7	3,606	154.7	98.9	34.6	16.5	5.5	14.2	3.8
	25	5,171	5.5	3,686	114.0	137.8	39.2	18.9	15.6	11.2	18.7
	26	5,184	4.8	2,535	109.9	108.8	35.7	11.1	16.3	7.6	16.0
	27	5,195	2.8	3,213	136.5	73.5	34.1	10.4	5.7	8.3	3.8
Woodford Shale	28	5,201	5.9	3,226	104.9	111.2	69.3	13.7	11.4	18.0	16.9
	29	5,210	2.1	2,921	182.9	52.6	45.7	21.6	6.4	15.5	3.5
	30	5,224	5.8	2,514	211.1	92.8	43.2	18.3	31.0	17.6	63.8
	31	5,248	9.0	1,935	217.5	57.1	53.2	23.0	26.6	29.8	40.6
	32	5,253	9.3	1,861	202.2	151.5	70.2	56.7	62.7	146.5	163.7
	33	5,262	9.4	2,278	184.4	131.4	63.5	35.4	57.7	68.7	110.3

Table 1 Continued

Interval	Sample	Depth	Na	Mg	Al	S	V	Cr	Fe	Zn	K
		ft.	ppm	ppm	ppm	ppm	ppm	ppm	ppm	ppm	ppm
Mississippian Limestone	1	4,968.5	6,246	5,794	33,959	6,002	30.6	312.9	17,464	141.1	15,261
	2	4,972	9,081	9,228	64,173	7,793	49.1	287.5	22,821	166.1	23,765
	3	4,973	7,435	9,175	56,962	9,618	48.0	258.1	23,744	99.8	25,105
	4	4,975	5,811	5,154	31,448	13,451	38.5	317.9	20,417	187.4	n.d.
	5	4,983	7,321	7,148	45,232	10,934	70.8	348.4	18,866	600.1	18,979
	6	4,992	7,786	8,475	43,146	12,634	207.3	323.9	21,208	370.6	19,115
	7	5,022	8,322	5,302	35,572	2,550	24.7	146.2	10,914	141.7	15,326
	8	5,033	6,805	11,908	36,531	9,261	58.3	180.2	21,421	213.6	15,454
	9	5,044	7,005	7,976	36,191	10,299	72.0	168.6	19,350	318.2	15,034
	10	5,050	6,691	6,908	45,249	8,407	80.2	386.6	18,064	289.7	22,124
	11	5,055	9,003	8,337	54,152	7,497	51.6	217.5	20,165	166.1	22,572
	12	5,059	10,046	7,176	59,686	7,921	57.3	224.6	22,852	139.5	22,779
	13	5,075	7,295	6,548	40,681	6,700	66.5	273.0	14,769	319.6	19,647
	14	5,086	7,591	7,154	46,807	7,797	40.5	132.0	18,586	165.6	20,444
	15	5,091	9,042	8,088	49,781	6,409	39.4	119.2	19,582	124.8	20,187
	16	5,099	6,688	11,498	33,570	7,084	32.8	133.0	17,441	94.9	13,896
	17	5,108	6,175	8,421	37,565	7,137	36.9	117.4	16,351	56.5	17,607
	18	5,112	6,376	9,226	44,323	6,827	62.8	175.6	16,676	153.8	20,557
	19	5,117	9,115	8,054	49,750	4,984	41.0	113.9	17,590	259.4	23,515
	20	5,120	8,599	7,386	57,280	6,863	48.3	151.0	21,760	239.6	20,820
	21	5,147	6,466	15,719	34,039	4,545	31.3	59.2	15,945	116.6	14,666
	22	5,150	4,217	23,913	24,235	4,973	23.3	55.0	17,759	86.1	10,509
	23	5,156	9,587	9,884	55,918	8,732	43.1	126.3	23,384	258.9	22,645
	24	5,160	8,170	9,044	52,640	7,923	44.5	137.2	23,947	163.1	24,807
	25	5,171	9,132	7,775	52,667	8,534	101.9	355.6	17,370	264.0	23,980
	26	5,184	5,477	6,621	33,648	7,374	89.5	213.2	13,007	336.3	14,928
	27	5,195	7,361	8,062	40,818	8,626	34.7	118.9	17,399	221.6	17,946
Woodford Shale	28	5,201	4,821	9,915	67,240	7,943	94.5	108.7	21,828	175.8	34,363
	29	5,210	4,214	12,558	61,373	6,763	90.2	76.4	22,239	73.1	30,308
	30	5,224	3,554	11,354	51,194	8,024	168.1	63.4	18,389	214.9	24,150
	31	5,248	2,868	10,279	40,602	19,139	64.6	46.1	23,148	47.9	20,979
	32	5,253	3,547	7,282	38,182	96,708	68.4	52.6	83,849	142.0	21,251
	33	5,262	4,452	11,734	45,671	52,518	76.4	50.1	53,253	100.2	24,103

Table 2: Trace element ratios for the core sample set.

Interval	Sample	Depth ft.	V/Ni	V/ (V+Ni)	U/Mo	V/Mo	Mo/Ni	U/Ni	V/Cr	Co/Ni	Ni/Co
Mississippian Limestone	1	4,968.5	0.6	0.4	0.9	7.6	0.1	0.1	0.1	0.1	8.0
	2	4,972	0.9	0.5	0.5	6.8	0.1	0.1	0.2	0.2	5.4
	3	4,973	0.9	0.5	0.5	7.1	0.1	0.1	0.2	0.2	5.0
	4	4,975	0.5	0.4	0.4	4.0	0.1	0.1	0.1	0.1	10.3
	5	4,983	0.5	0.3	0.8	3.8	0.1	0.1	0.2	0.1	13.6
	6	4,992	1.8	0.6	0.7	8.6	0.2	0.1	0.6	0.1	11.1
	7	5,022	0.8	0.5	2.1	15.2	0.1	0.1	0.2	0.2	5.1
	8	5,033	0.8	0.4	0.9	4.5	0.2	0.2	0.3	0.1	7.2
	9	5,044	1.1	0.5	0.9	5.8	0.2	0.2	0.4	0.1	7.4
	10	5,050	0.5	0.3	0.8	3.5	0.1	0.1	0.2	0.1	15.0
	11	5,055	0.7	0.4	1.0	6.1	0.1	0.1	0.2	0.2	5.6
	12	5,059	0.9	0.5	0.8	6.1	0.1	0.1	0.3	0.2	4.8
	13	5,075	0.5	0.3	1.3	4.9	0.1	0.1	0.2	0.1	12.2
	14	5,086	0.8	0.4	1.4	9.8	0.1	0.1	0.3	0.2	4.8
	15	5,091	0.7	0.4	1.3	9.1	0.1	0.1	0.3	0.2	4.5
	16	5,099	0.8	0.4	1.3	9.8	0.1	0.1	0.2	0.3	3.8
	17	5,108	0.8	0.4	1.6	10.0	0.1	0.1	0.3	0.2	4.6
	18	5,112	0.8	0.4	1.2	7.8	0.1	0.1	0.4	0.2	6.5
	19	5,117	0.8	0.4	3.0	29.2	0.0	0.1	0.4	0.2	4.7
	20	5,120	0.6	0.4	1.4	11.7	0.0	0.1	0.3	0.1	6.9
	21	5,147	2.1	0.7	3.6	37.6	0.1	0.2	0.5	0.5	2.2
	22	5,150	0.8	0.4	4.3	34.8	0.0	0.1	0.4	0.2	4.2
	23	5,156	0.5	0.3	1.4	11.1	0.0	0.1	0.3	0.2	5.6
	24	5,160	0.4	0.3	1.4	11.6	0.0	0.1	0.3	0.1	7.0
	25	5,171	0.7	0.4	0.8	5.4	0.1	0.1	0.3	0.1	12.3
	26	5,184	0.8	0.5	1.0	5.6	0.1	0.1	0.4	0.1	14.4
	27	5,195	0.5	0.3	1.5	9.3	0.1	0.1	0.3	0.1	8.8
Woodford Shale	28	5,201	0.8	0.5	0.7	5.6	0.2	0.1	0.9	0.2	6.2
	29	5,210	1.7	0.6	1.9	26.0	0.1	0.1	1.2	0.3	3.4
	30	5,224	1.8	0.6	0.5	2.6	0.7	0.3	2.7	0.2	5.3
	31	5,248	1.1	0.5	0.7	1.6	0.7	0.5	1.4	0.5	1.9
	32	5,253	0.5	0.3	0.4	0.4	1.1	0.4	1.3	1.0	1.0
	33	5,262	0.6	0.4	0.5	0.7	0.8	0.4	1.5	0.5	1.9

Table 3: Major and trace element enrichment factors for the core sample set (n.d. means not determined).

Interval	Sample	Depth	Ti	Mn	Ni	Cu	Pb	U	Co	Mo
		ft.	EF	EF	EF	EF	EF	EF	EF	EF
Mississippian Limestone	1	4,968.5	1.9	1.0	6.2	2.4	3.3	3.1	1.6	6.4
	2	4,972	1.6	0.3	3.5	1.4	1.3	1.6	1.3	6.0
	3	4,973	1.6	0.5	3.8	1.4	1.6	1.8	1.5	6.4
	4	4,975	2.0	0.8	9.0	3.2	2.6	3.8	1.8	16.3
	5	4,983	1.8	0.5	12.1	3.2	1.2	9.2	1.8	21.8
	6	4,992	1.9	0.6	10.8	2.7	1.8	11.4	1.9	30.0
	7	5,022	2.4	0.4	3.3	1.5	1.1	2.8	1.3	2.5
	8	5,033	2.0	1.0	8.1	2.0	1.5	9.1	2.3	19.0
	9	5,044	1.6	0.7	7.3	2.0	1.5	8.6	2.0	18.3
	10	5,050	1.8	0.4	15.4	4.2	1.7	11.6	2.0	27.2
	11	5,055	1.7	0.4	5.3	1.8	1.2	4.3	1.9	8.4
	12	5,059	1.9	0.3	4.5	1.7	1.2	3.8	1.9	8.4
	13	5,075	1.5	0.4	12.9	2.8	1.4	12.8	2.1	17.8
	14	5,086	2.0	0.4	4.5	1.5	1.3	3.4	1.9	4.7
	15	5,091	1.9	0.4	4.3	2.0	1.2	3.3	1.9	4.7
	16	5,099	2.2	0.8	5.0	1.9	1.5	3.7	2.6	5.4
	17	5,108	2.1	0.6	4.9	1.7	1.5	4.4	2.1	5.3
	18	5,112	1.8	0.5	7.3	1.9	1.4	6.0	2.2	9.8
	19	5,117	2.0	0.4	4.3	2.5	1.2	2.4	1.8	1.5
	20	5,120	1.9	0.3	6.0	2.6	1.1	3.0	1.7	3.9
	21	5,147	2.0	0.9	1.7	1.1	1.4	2.5	1.6	1.3
	22	5,150	2.3	1.8	4.8	1.9	1.4	3.4	2.2	1.5
	23	5,156	1.9	0.4	5.9	2.5	1.3	2.9	2.1	3.7
	24	5,160	1.8	0.4	7.6	2.1	1.3	3.0	2.2	3.9
	25	5,171	1.9	0.3	10.5	2.4	1.4	8.5	1.7	19.0
	26	5,184	2.0	0.4	13.0	3.4	1.3	13.9	1.8	25.5
	27	5,195	2.1	0.4	7.2	2.7	1.0	4.0	1.6	4.9
Woodford Shale	28	5,201	1.3	0.2	6.6	3.3	0.8	4.9	2.2	13.4
	29	5,210	1.3	0.4	3.4	2.4	1.4	3.0	2.0	3.0
	30	5,224	1.3	0.6	7.3	2.7	1.4	17.4	2.8	66.8
	31	5,248	1.3	0.7	5.7	4.2	2.3	18.8	5.9	53.7
	32	5,253	1.3	0.7	16.0	5.9	6.0	47.1	30.9	229.8
	33	5,262	1.3	0.5	11.6	4.5	3.1	36.3	12.1	129.4

Table 3 Continued

Interval	Sample	Depth	Na	Mg	S	V	Cr	Fe	Zn	K
		ft.	EF	EF	EF	EF	EF	EF	EF	EF
Mississippian Limestone	1	4,968.5	0.5	1.0	6.5	1.2	21.2	1.2	4.7	1.3
	2	4,972	0.4	0.9	4.5	1.0	10.3	0.8	2.9	1.1
	3	4,973	0.4	1.0	6.3	1.1	10.4	1.0	2.0	1.3
	4	4,975	0.5	1.0	15.8	1.6	23.2	1.5	6.7	n.d.
	5	4,983	0.5	1.0	9.0	2.1	17.7	1.0	15.0	1.2
	6	4,992	0.5	1.2	10.8	6.4	17.2	1.1	9.7	1.3
	7	5,022	0.7	0.9	2.7	0.9	9.4	0.7	4.5	1.2
	8	5,033	0.5	2.0	9.4	2.1	11.3	1.3	6.6	1.2
	9	5,044	0.5	1.3	10.5	2.7	10.7	1.2	10.0	1.2
	10	5,050	0.4	0.9	6.9	2.4	19.6	0.9	7.2	1.4
	11	5,055	0.5	0.9	5.1	1.3	9.2	0.9	3.5	1.2
	12	5,059	0.5	0.7	4.9	1.3	8.6	0.9	2.6	1.1
	13	5,075	0.5	1.0	6.1	2.2	15.4	0.8	8.9	1.4
	14	5,086	0.5	0.9	6.2	1.2	6.5	0.9	4.0	1.3
	15	5,091	0.5	1.0	4.8	1.1	5.5	0.9	2.8	1.2
	16	5,099	0.6	2.1	7.8	1.3	9.1	1.2	3.2	1.2
	17	5,108	0.5	1.4	7.0	1.3	7.2	1.0	1.7	1.3
	18	5,112	0.4	1.3	5.7	1.9	9.1	0.9	3.9	1.3
	19	5,117	0.5	1.0	3.7	1.1	5.3	0.8	5.9	1.4
	20	5,120	0.4	0.8	4.4	1.1	6.1	0.9	4.7	1.0
	21	5,147	0.5	2.8	4.9	1.2	4.0	1.1	3.9	1.2
	22	5,150	0.5	6.0	7.6	1.3	5.2	1.7	4.0	1.2
	23	5,156	0.5	1.1	5.8	1.0	5.2	1.0	5.2	1.2
	24	5,160	0.4	1.0	5.6	1.1	6.0	1.0	3.5	1.4
	25	5,171	0.5	0.9	6.0	2.6	15.5	0.8	5.7	1.3
	26	5,184	0.5	1.2	8.1	3.6	14.6	0.9	11.3	1.3
	27	5,195	0.5	1.2	7.8	1.1	6.7	1.0	6.1	1.3
Woodford Shale	28	5,201	0.2	0.9	4.4	1.9	3.7	0.7	3.0	1.5
	29	5,210	0.2	1.2	4.1	2.0	2.9	0.8	1.3	1.4
	30	5,224	0.2	1.3	5.8	4.4	2.8	0.8	4.8	1.4
	31	5,248	0.2	1.5	17.5	2.1	2.6	1.3	1.3	1.5
	32	5,253	0.3	1.2	93.8	2.4	3.2	5.0	4.2	1.6
	33	5,262	0.3	1.6	42.6	2.2	2.5	2.7	2.5	1.5

4.2 Oil Samples

Tables 4 and 5 show the elemental concentrations and the trace element ratios, respectively, for the oil samples used in this study. Multiple elemental concentrations for the whole oil samples could not be determined, as noted in Table 5.

Table 4: Major and trace elements for the oil sample set (n.d. means not determined).

Sample	County	Ti	Mn	Ni	Cu	U	Co	Mo	Na
		ppm	ppm	ppm	ppm	ppm	ppm	ppm	ppm
CW	Blaine	0.7	1.0	n.d.	n.d.	0.03	0.01	0.12	9.2
HW	Logan	0.3	0.2	1.0	n.d.	0.03	0.02	0.01	5.0
WW	Logan	0.6	0.2	0.6	0.3	0.03	0.04	0.03	35.5
PW	Payne	1.5	0.1	1.0	0.1	0.03	0.03	0.03	11.0
MW	Logan	2.8	0.1	0.8	0.2	0.03	0.05	0.06	17.9
WO1	Lincoln	n.d.	0.3	7.8	0.3	0.03	0.06	0.02	22.9
WO2	Lincoln	n.d.	0.2	14.4	3.3	0.03	0.05	0.02	24.8
WO3	Lincoln	0.4	0.0	4.3	0.4	0.02	0.02	0.01	5.5
WO4	Payne	1.0	0.4	0.9	0.2	0.02	8.43	0.01	15.1
WO5	Woods	n.d.	0.1	105.5	0.5	0.03	0.17	0.06	19.9
WO6	Alfalfa	2.2	0.2	10.5	0.7	0.04	0.17	0.02	30.9

Sample	County	Mg	Al	Ca	V	Cr	Fe	Zn	K
		ppm	ppm	ppm	ppm	ppm	ppm	ppm	ppm
CW	Blaine	9.1	n.d.	5.2	n.d.	1.1	23.0	n.d.	n.d.
HW	Logan	0.2	3.0	38.3	n.d.	1.4	5.5	5.6	0.04
WW	Logan	0.6	66.1	2.9	0.25	n.d.	1.5	1.0	2.03
PW	Payne	n.d.	n.d.	n.d.	0.70	3.3	14.1	0.7	0.25
MW	Logan	0.8	3.5	40.5	0.10	3.0	29.7	3.1	1.94
WO1	Lincoln	2.9	4.1	171.4	6.16	2.3	18.8	17.9	2.53
WO2	Lincoln	2.7	32.4	124.9	10.76	2.5	14.8	16.6	0.42
WO3	Lincoln	n.d.	5.4	6.1	0.92	0.7	9.5	1.7	n.d.
WO4	Payne	2.6	14.0	94.9	0.02	1.2	8.3	13.1	2.02
WO5	Woods	1.9	41.1	65.0	318.89	2.7	22.1	15.7	30.26
WO6	Alfalfa	2.4	15.5	113.0	27.99	1.9	24.2	19.6	30.01

Table 5: Trace element ratios for the oil sample set (n.d. means not determined).

Sample	County	V/Ni	Mo/Ni	U/Ni	Co/Ni	Cu/Ni	V/(V+Ni)	U/Mo	V/Mo	Ni/Co
CW	Blaine	n.d.	n.d.	n.d.	n.d.	n.d.	n.d.	0.3	n.d.	n.d.
HW	Logan	n.d.	0.007	0.0308	0.019	n.d.	n.d.	4.6	n.d.	53.2
WW	Logan	0.41	0.045	0.0561	0.072	0.471	0.29	1.2	9.1	13.8
PW	Payne	0.70	0.034	0.0295	0.030	0.064	0.41	0.9	20.6	33.2
MW	Logan	0.12	0.073	0.0333	0.060	0.219	0.10	0.5	1.6	16.8
WO1	Lincoln	0.79	0.002	0.0041	0.007	0.038	0.44	1.8	345.1	140.4
WO2	Lincoln	0.75	0.001	0.0023	0.003	0.229	0.43	2.0	637.0	308.6
WO3	Lincoln	0.22	0.002	0.0056	0.006	0.089	0.18	3.5	134.4	176.2
WO4	Payne	0.03	0.013	0.0229	9.157	0.178	0.03	1.8	2.1	0.1
WO5	Woods	3.02	0.001	0.0003	0.002	0.004	0.75	0.5	5132.1	612.5
WO6	Alfalfa	2.68	0.002	0.0038	0.016	0.066	0.73	1.7	1200.4	61.1

CHAPTER V

DISCUSSION

5.1 Trace Elements

Measurement of trace elements for the analysis of source rocks and crude oils has been used for many years but has developed significantly over the recent 10-20 years. Specific elements, including V, Ni, Mo, Co, Cu and U, have been found to have significant association with organic matter, and are sensitive indicators for paleoredox conditions. Furthermore, the elemental ratios of these redox-sensitive elements are stable within reservoirs and source rocks, even under changing conditions such as oxidation, biodegradation, generation and migration (McManus et al., 1999; Jin et al., 2001; Morford et al., 2001; Algeo and Maynard, 2004; Harris et al., 2004; Tribovillard et al., 2006; Jiao et al., 2010; MacDonald et al., 2010; Fu et al., 2011; Adegoke et al., 2014). Each of these elements, except for U, are transition metals that have been studied previously to ascertain source rock organic matter input, paleoredox conditions and depositional environments of rock units and, even the origin, maturation and migration events of crude oils (Barwise, 1990; Hirner and Xu, 1991; Udo et al., 1992; Nwachukwu et al., 1995; Lo Monaco et al., 2002; Akinlua et al., 2007b; Galarraga et al., 2008; Akinlua and Torto, 2011; Adegoke et al., 2014).

Here, in discussing our paleo-depositional and –redox conditions, we use the classification scheme summarized in Tribovillard et al. (2006), which divides oxygenation environments into four zones: oxic, suboxic, anoxic, and euxinic (Table 6). In this way, we remain consistent, when describing out results and interpretations, with the majority of studies in the literature.

Table 6: Redox classification of the depositional environments, after Tyson and Pearson (1991), reprinted from Tribovillard et al. (2006).

Redox classes	Oxic	Suboxic	Anoxic	Euxinic
			No free H_2S in the water column	Free H_2S present in the water column
O_2 concentration in bottom waters (ml O_2/l H_2O)	$[O_2]>2$	$2>[O_2]>0.2$	$[O_2]<0.2$	$[O_2]=0$

The values for O_2 concentrations in bottom waters are valid for present-day ocean.

5.2 Core Sample Analysis

A number of previous studies (Lewan, 1984; Akinlua et al., 2007a; Akinlua et al., 2007b; Akinlua et al., 2010; Akinlua, 2011; Adegoke et al., 2014; Gao et al., 2015; Akinlua et al., 2016; Lopez and Lo Monaco, 2017) have shown that source rock type, organic matter type and the environment of deposition have profound effects on the concentration of trace elements in source rocks. In this study, core samples were analyzed using trace element ratios and trace element enrichment factors (EFs), along with TOC, to determine organic matter type, paleo-redox conditions and depositional environments.

5.2.1 Trace Element Ratios for Organic Matter Classification

Multiple studies, such as those by Barwise (1990), Galarraga et al. (2008), Akinlua et al. (2010), Adegoke et al. (2014) and Akinlua et al. (2016), have used trace element ratios for the classification of organic matter in source rocks. These studies have shown that V/Ni ratios higher than 3 indicate marine organic input, V/Ni ratios from 1.9 to 3 indicate mixed terrigenous and marine organic input, and V/Ni ratios less than 1.9 indicate predominantly terrigenous organic input. Figure 6 shows the Woodford Shale and the Mississippian Limestone samples with V

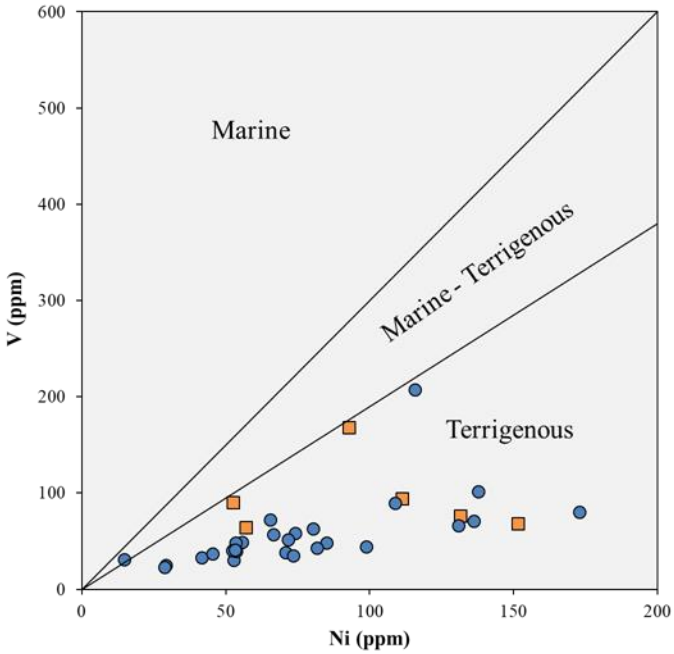

Figure 6: V vs. Ni for the Woodford Shale (orange squares) and the Mississippian Limestone (blue circles) core samples (Galarraga et al., 2008).

plotted against Ni (modified after Galarraga et al., 2008). In this study, the V/Ni ratios for both units are quite low. While the Woodford Shale V/Ni ratios do not exceed 1.81, the Mississippian Limestone cores contain only one sample whose V/Ni ratio does exceed the 1.9 threshold (2.13, samples 21), entering the mixed marine-terrestrial field established by Galarraga et al. (2008). These low V/Ni ratios indicate that the dominant organic matter input for these Woodford Shale and Mississippian Limestone core samples was from a predominantly terrigenous source.

Additionally, others (Nwachukwu et al., 1995; Galarraga et al., 2008; Akinlua et al., 2010; Akinlua and Torto, 2011; Akinlua et al., 2016) explain that, besides V/Ni, Co/Ni ratios are useful in determining organic matter source because Co/Ni ratios also are likely to remain unchanged by diagenetic effects. V/Ni and Co/Ni, when used in conjunction with one another,

can better constrain the organic matter source. Akinlua and Torto (2011) explain that samples with high V/Ni ratio and low Co/Ni ratio are suggestive of terrigenous organic matter input, samples with comparative intermediate values of V/Ni ratio and Co/Ni ratio suggest mixed organic matter input, and samples with low V/Ni ratio and high Co/Ni ratio suggest marine organic matter input (Udo et al., 1992).

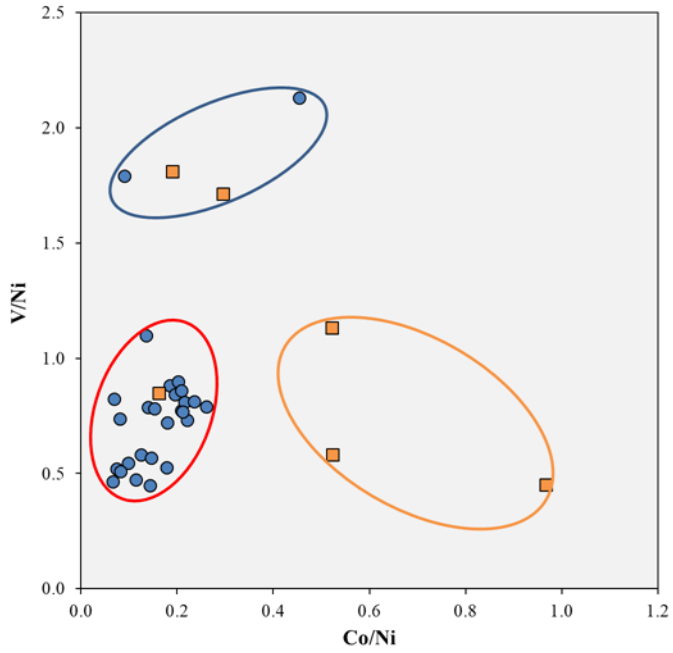

Figure 7: V/Ni vs. Co/Ni for the Woodford Shale (orange squares) and the Mississippian Limestone (blue circles) core samples. The red oval represents predominantly terrigenous input, the blue oval represents mixed marine and terrigenous input and the orange oval represents a predominantly marine input.

Figure 7 shows V/Ni vs. Co/Ni for the Woodford Shale and Mississippian Limestone core samples. From this figure we suggest that: 1) 25 of the Mississippian Limestone samples and only 1 of the Woodford Shale samples (28) have low values of both Ni/V and Co/V (red

oval), indicating predominantly terrigenous organic matter, 2) 2 of the Mississippian Limestone samples (6 and 21) and 2 of the Woodford Shale samples (29 and 30) have relatively high V/Ni values and intermediate Co/Ni values (blue oval), indicating mixed, but predominantly terrigenous, organic matter, and 3) 3 of the Woodford Shale samples (31, 32 and 33) and none of the Mississippian Limestone samples have high Co/Ni values and low V/Ni values (orange oval), indicating predominantly marine organic matter.

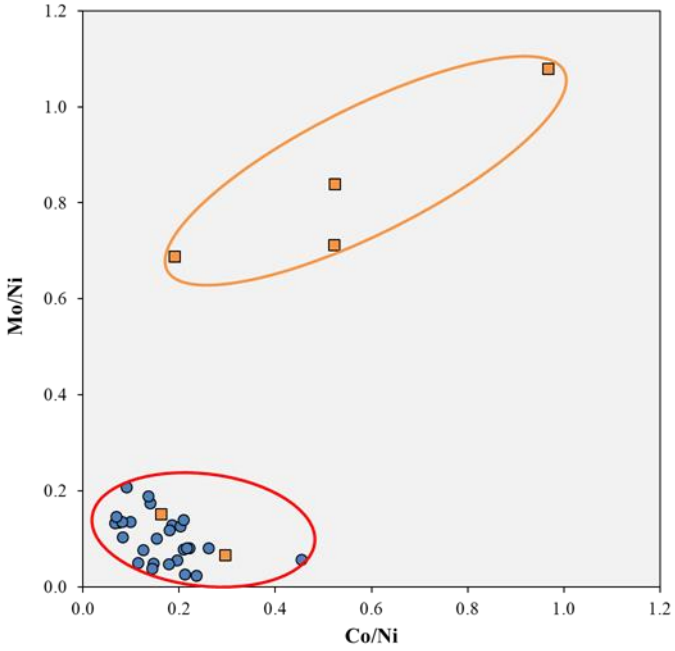

Figure 8: Mo/Ni vs. Co/Ni for the Woodford Shale (orange squares) and the Mississippian Limestone (blue circles) core samples. The red oval represents a terrigenous organic matter source and the orange oval represents a marine organic matter source.

Akinlua et al. (2010) show that Mo/Ni has a good positive correlation with Co/Ni, indicating that it, too, can be a useful tool as an organic matter source indicator. They explain

that, as found for the Co/Ni ratio, increasing Mo/Ni ratios suggest an increase of marine organic matter. Figure 8 shows the Mo/Ni and Co/Ni ratios for the Mississippian Limestone and Woodford Shale samples. From this figure, we can see two distinct groups have formed which include 1) all 27 Mississippian Limestone samples and 2 Woodford Shale samples (28 and 29) (low Mo/Ni and low Co/Ni) (red oval) and 2) 4 of the Woodford Shale samples (30, 31, 32 and 33) (high Mo/Ni and high Co/Ni) (blue oval). Since the Co/Ni and Mo/Ni ratios increase with increasing marine organic matter input, we interpret that 1) the Mississippian Limestone samples and the two Woodford samples share a common terrigenous organic matter input and/or were deposited in less reducing conditions and 2) the 4 Woodford Shale samples share a common marine organic matter type and/or were deposited in more reducing conditions.

In comparing our interpretations from the V/Ni, Co/Ni and Mo/Ni ratios, we can attempt to better group the samples based on organic matter input. From Figure 6, we have determined that all of the samples had terrigenous-derived organic matter. From Figure 7, we determined that 3 Woodford samples contained marine-derived organic matter, and that 1 Woodford sample and 25 Mississippian samples had terrigenous-derived organic matter. Finally, we suggested that 2 Woodford samples and 2 Mississippian samples contained mixed organic matter from both terrigenous and marine sources. From the Mo/Ni vs. Co/Ni values, we determined that 4 Woodford samples contained marine-derived organic matter and that 2 Woodford samples and all 27 Mississippian samples had terrigenous-derived organic matter.

Although these interpretations are not perfectly consistent, for the most part, they suggest a common derivation of terrigenous organic matter for the great majority of the samples. A possible explanation for the small disagreement between these figures is that the Co/Ni and Mo/Ni ratios are actually indicating the paleoredox conditions during the deposition of the

organic matter, while the V/Ni ratios truly indicate the type of organic matter that was deposited in this area (further discussed below).

5.2.2 Trace Element Ratios for Paleoredox Determination

In a methodology first developed by Lewan (1984) and used in a number of previous studies (Hatch and Leventhal, 1992; Rimmer, 2004; Galarraga et al., 2008; Akinlua et al., 2010; Adegoke et al., 2014; Lopez and Lo Monaco, 2017), V, Ni, and S concentration relationships were used to determine a paleoredox classification scheme. Since the proportionality of V and Ni are sensitive to redox conditions, the depositional environments of the core samples can be determined. This scheme is divided into three regimes based on (V/V+Ni)) and S content.

Lewan (1984) explains that, within this methodology, three regimes exist which represent differing paleoredox conditions. Regime I represents conditions where V occurs as quinquivalent, causing vanadyl cations to not be available for metalation. However, Ni cations would be available for metalation and the proportionality of V to Ni is low ($V/(V+Ni) < 0.10$) in the organic matter which also contains low sulfur content (Lewan, 1984). Regime II represents conditions in which both V and Ni cations are available for metalation, and the proportionality of V to Ni ($V/(V+Ni)$) is < 0.5, with sulfur contents that are low (Lewan, 1984). The variety of controls on the V-Ni fractions in organic matter, in this regime, suggests that a high variability of V-Ni fractions may be expected not only in rocks from different units, but also in rocks from the same unit but different horizons (Lewan, 1980; Lewan, 1984). Regime III is only present if there is a significant quantity of sulfate-reducing bacteria operating in the sediment, allowing for all of the sulfate in a marine system to be reduced (high sulfur content) (Lewan, 1984). The availability of Ni cations is then reduced in Regime III by the formation of aqueous sulfide

complexes and the V-Ni fraction should be greater than 0.5 due to this reduction in Ni cations and the availability of V cations (Lewan, 1984).

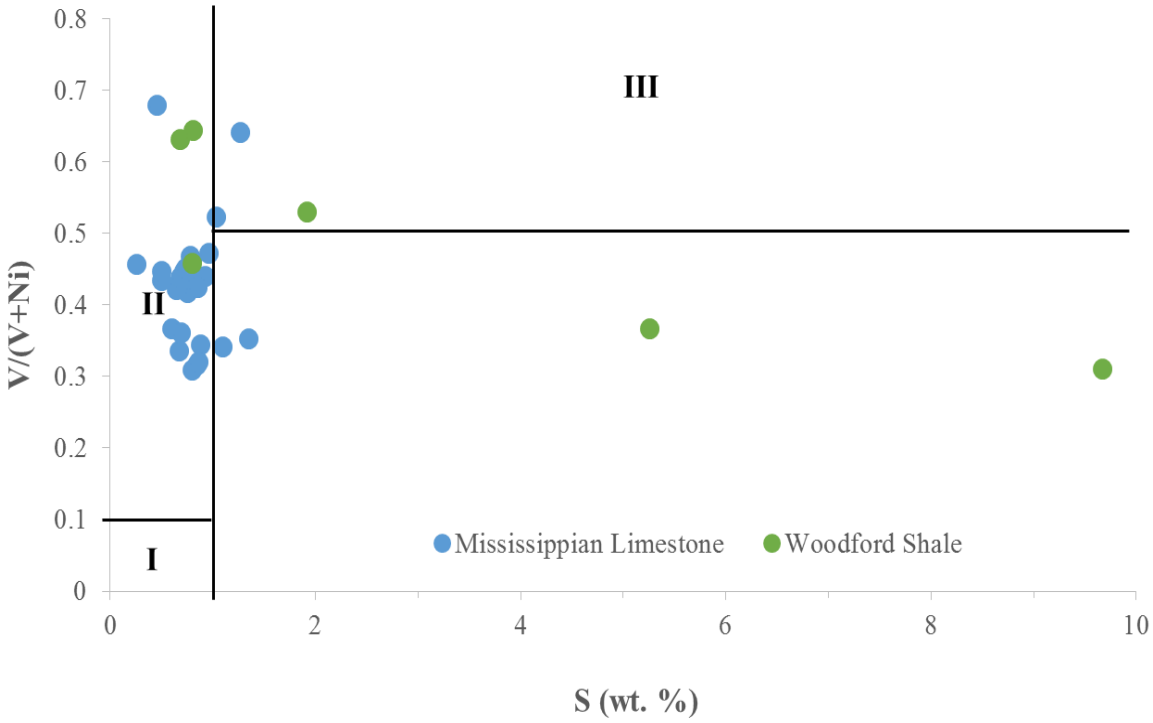

Figure 9: Lewan (1984) diagram for all core samples in this study.

Studies completed by Nwachukwu et al. (1995), Akinlua et al. (2007a and b), Akinlua and Torto (2011), Mudiaga (2011), Akinlua et al., (2015), Gao et al. (2015), Akinlua et al. (2016), Lopez and Lo Monaco (2017) and Zhao et al. (2017) have shown that the V/(V+Ni) ratios in organic matter can be accurately used to determine the paleoredox conditions present at the time of the organic matter deposition. Figures 9, 10 and 11 show plots of the total 33 samples, the 6 Woodford samples and the 27 Mississippian Limestone samples, respectively, using the classification scheme developed by Lewan (1984). For the Woodford Shale interval (a

total of 6 samples), we suggest a paleoredox environment consistent with suboxic-anoxic conditions for the samples (28, 29 and 30) that plot in Regime II. Sample 31 plots in Regime III, indicating an anoxic-euxinic environment. Samples 32 and 33 do not fall within the Regime thresholds, suggesting that these samples were deposited in a highly anoxic-euxinic environment (Fig. 10).

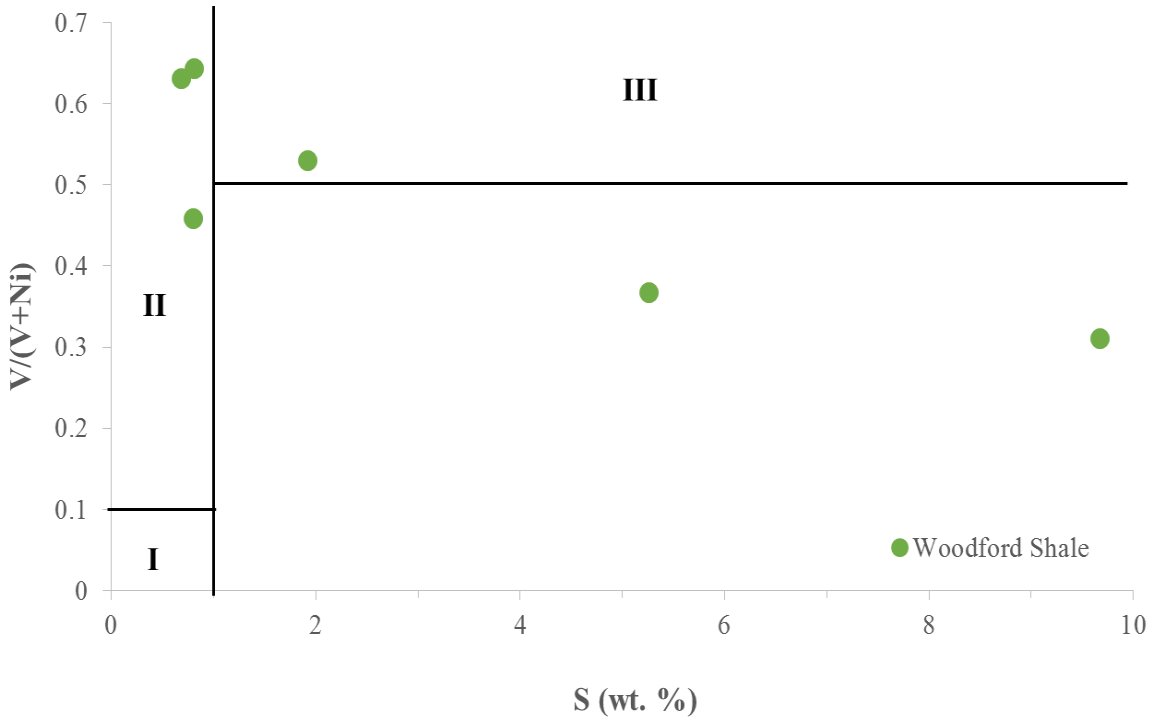

Figure 10: Lewan (1984) diagram for core samples from the Woodford Shale.

For the Mississippian Limestone interval, 23 samples (1-3, 7, 8, 10-27) fall within Regime II, suggesting suboxic-anoxic conditions (Fig. 11). Samples 6 and 9 fall within Regime III and suggest an anoxic-euxinic environment. Samples 4 and 5 fall outside of the range of

given values for the three regimes. The low sulfur content of these samples suggests that they were likely deposited in suboxic-anoxic conditions.

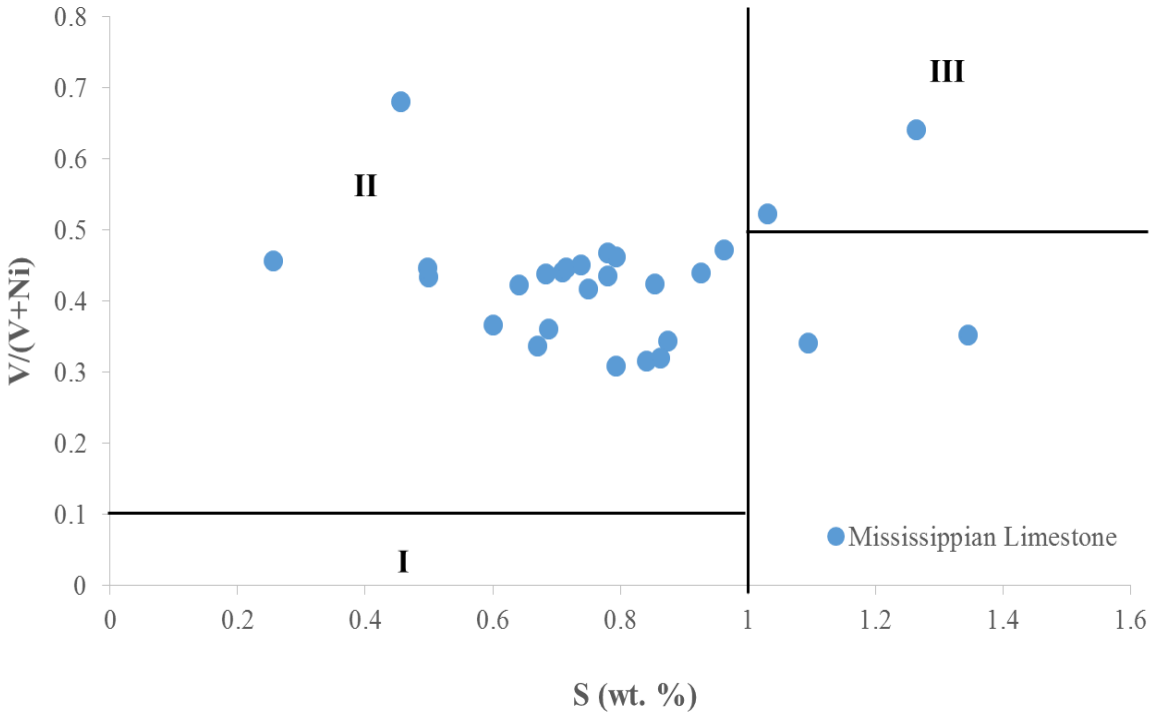

Figure 11: Lewan (1984) diagram for core samples from the Mississippian Limestone.

5.2.3 Trace Element EFs for Paleoredox and Depositional Environment Determination

Trace element EFs have been extensively used in previous studies to mainly determine the paleo-redox conditions, but also to help in establishing overall depositional environments of core samples (Van der Weijden, 2002; Algeo and Maynard, 2004; Brumsack, 2006; Tribovillard et al., 2006; Piper et al., 2007; Tribovillard et al., 2008; Little et al., 2015). EFs, however, cannot be determined for oil samples because no reference material exists and the trace element

concentrations within oils change during in-reservoir alteration events. Therefore, EFs were only calculated for the rock samples.

In order to use the EF tool, the first step is to evaluate the concentrations in each sample relative to the concentrations in a reference material. This can be done by normalizing the trace metal concentration to Al content, in both the sample and the reference material, and then comparing the two normalized values. Tribovillard et al. (2006) explains that Al content can be used here because it represents the aluminosilicate fraction, or detrital contribution, in the sediments, with very little ability to change during alterations events, such as diagenesis (Brumsack, 1989; Calvert and Pederson, 1993; Morford and Emerson, 1999; Piper and Perkins, 2004). To complete this comparison, we use the equation:

$$EF_{\text{element X}} = (X/Al)_{\text{sample}} / (X/Al)_{\text{reference material}}. \qquad (1)$$

Where X is the element of choice. Algeo and Tribovillard (2009) explain that, in practice, a detectable authigenic enrichment corresponds to an EF > 3 and a substantial authigenic enrichment corresponds to an EF > 10. Therefore, an EF < 3 indicates authigenic depletion of the element, relative to the reference material. The most commonly used reference material, and the one used here for direct comparison, is average upper continental crustal rocks.

Although, the above-mentioned EF determination method is easy and quick to complete, there are some drawbacks. Tribovillard et al. (2006) and Van der Weijden (2002) explain that some trace metal concentrations may need to be modified before using this method. If left unmodified, the calculated EFs will be unreliable. This will likely occur if the coefficient of variation of the Al concentration is large compared to the coefficient of variation of the chosen elements (Van der Weijden, 2002; Tribovillard et al., 2006). The samples analyzed in this study

do not show a large difference between the coefficient of variation of Al and the chosen elements.

Using the redox-sensitive trace metals Ni, Cu, Zn, Cr, Co, V, Mo, and U, Tribovillard et al. (2006) determined a methodology to interpret paleoenvironmental deposition histories. Tribovillard et al. (2006) explain the reasoning behind their methodology as follows: 1) U, V and Mo behave as redox proxies with minimal detrital influences, 2) Cr and Co behave as redox proxies with a strong detrital influence and 3) Ni, Cu and Zn behave as productivity proxies. A caveat to the use of this scheme, however, is that some of the elements are influenced by additional sources. Here we use a variety of trace element EFs, much in the same vein as Tribovillard et al. (2006), to interpret the paleoenvironmental and depositional histories of the Woodford Shale and Mississippian carbonate samples. For the determination of paleoredox conditions of the core samples, trace element EFs were calculated using the above-mentioned method.

5.2.3a U, V and Mo

Throughout the entire core interval, U EFs range from 1.6 to 47.1, V EFs range from 0.9 to 6.4 and Mo EFs range from 1.3 to 229.8 (Figures 12 and 13). The fact that we have enrichment, to various degrees, of each of these three elements, suggests that the paleoredox conditions during deposition of this core interval were anoxic to some extent. Greater enrichment of Mo, especially, suggests the presence of H_2S and, therefore, euxinic conditions.

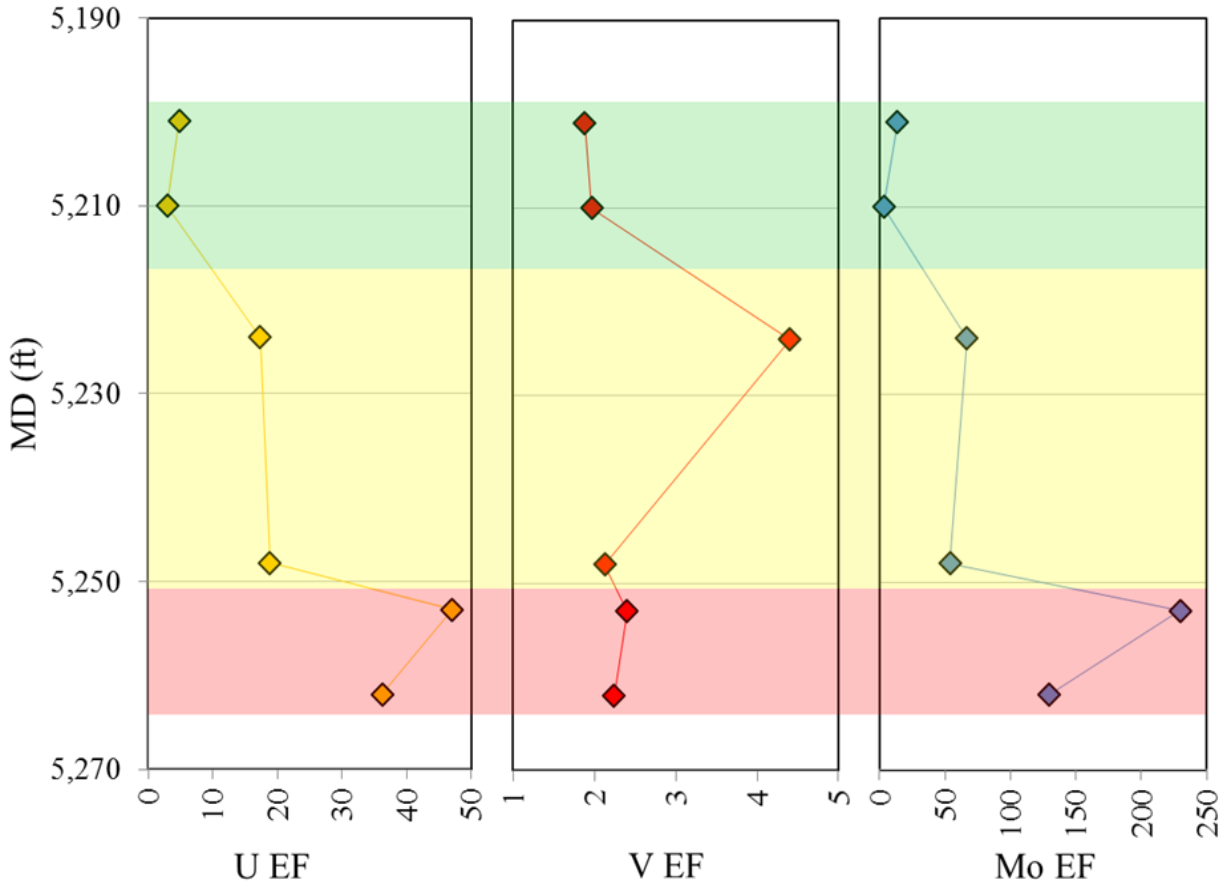

Figure 12: U, V and Mo enrichment factors (EFs) for the Woodford Shale core samples. Group 1 (Green) represents anoxic-suboxic conditions, Group 2 (Yellow) represents anoxic-euxinic conditions and Group 3 (Red) represents highly anoxic-euxinic conditions.

Within the Woodford Shale interval (5,201'-5,262'), U EFs range from 3.0 to 47.1, V EFs range from 1.9 to 4.4 and Mo EFs range from 3.0 to 229.8. This interval, which contains 6 total samples, was divided into 3 groups using U, V and Mo EFs. These groups are shown in Figure 12 and include: Group 1 (Green): samples 28 and 29 (U EFs range: 3.0-4.9; V EFs range: 1.9-2.0; Mo EFs range: 3.0-13.4), Group 2 (Yellow): samples 30 and 31 (U EFs range: 17.4-18.8; V EFs range: 2.1-4.4; Mo EFs range: 53.7-66.9) and Group 3 (Red): samples 32 and 33 (U EFs range: 36.3-47.1; V EFs range: 2.2-2.4; Mo EFs range 129.4-229.8). We interpret Group 1

(Green) to represent suboxic-anoxic conditions, Group 2 (Yellow) anoxic-euxinic conditions, and Group 3 (Red) highly anoxic-euxinic conditions (Figure 12). It is the extreme enrichment factors for Mo that suggest an extremely euxinic environment for Group 3 samples, and the lower enrichment factors that suggest an anoxic environment, but with much lower or non-existent levels of euxinia, indicating suboxic-anoxic conditions for the Group 1 samples. The only small issue, regarding V EFs, arises between group 2 and 3, where sample 31 falls in group 3 for V EFs, rather than group 2, as seen for U and Mo EFs.

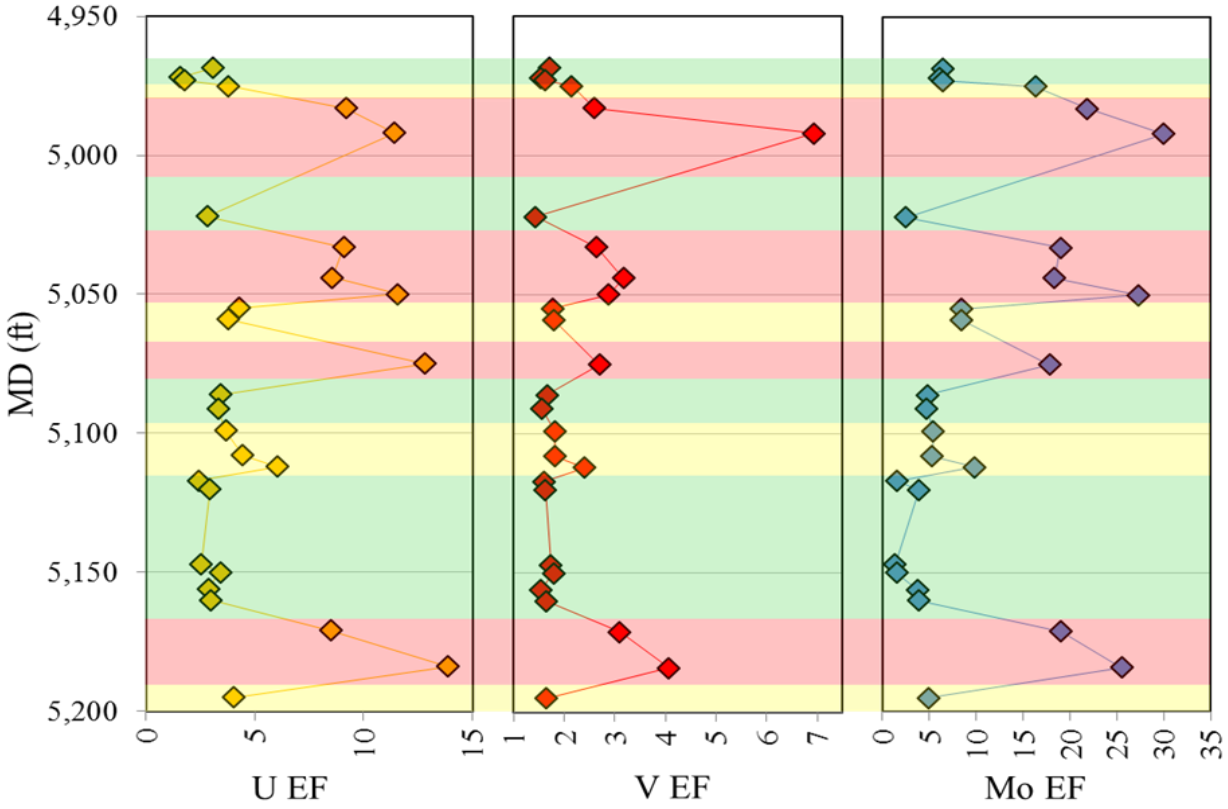

Figure 13: U, V and Mo enrichment factors (EFs) for the Mississippian Limestone core samples. Group 1 (Green) represents suboxic-anoxic conditions, Group 2 (Yellow) represents more anoxic conditions and Group 3 (Red) represents anoxic-euxinic conditions.

Within the Mississippian Limestone interval (4,962.5'-5,195'), U EFs range from 1.6 to 13.9, V EFs range from 0.9 to 6.4 and Mo EFs range from 1.3 to 29.9 (Figure 13). The 27 samples within this interval were divided into the same three paleoenvironmental depositional groups identified in the Woodford samples using redox-sensitive U, V, and Mo EFs. These groups are shown in Figure 13 and include: Group 1 (Green; suboxic to anoxic): samples 1-3, 7, 14, 15 and 19-24 (U EFs range: 0-3.5; V EFs range: 0-1.3; Mo EFs range: 0-6.5), Group 2 (Yellow; anoxic): samples 4, 11, 12, 16-18 and 27 (U EFs range: 3.5-6.5; V EFs range: 1.14-1.89; Mo EFs range: 4.9-16.5), and Group 3 (Red; anoxic-euxinic): samples 5, 6, 8-10, 13, 25 and 26 (U EFs range: >6.5; V EFs range: >1.89; Mo EFs range >16.5).

5.2.3b Ni and Cu

Ni EFs range from 1.7 to 15.9 and Cu EFs range from 1.1 to 5.9, throughout the entire interval (Figure 14 and 15). Ni and Cu are dominantly delivered to sediments in association with organic matter (Tribovillard et al., 2006). Tribovillard et al. (2006) explains that Ni and Cu are released to the sediment through organic matter decay and often become trapped by pyrite in sulfate-reducing conditions and that high Ni and Cu content indicate that 1) a high organic matter flux supplied these elements to the sediment and 2) reducing conditions were met. The association of Ni and Cu with organic matter, thus, allows high-productivity environments to be determined using Ni and Cu EFs.

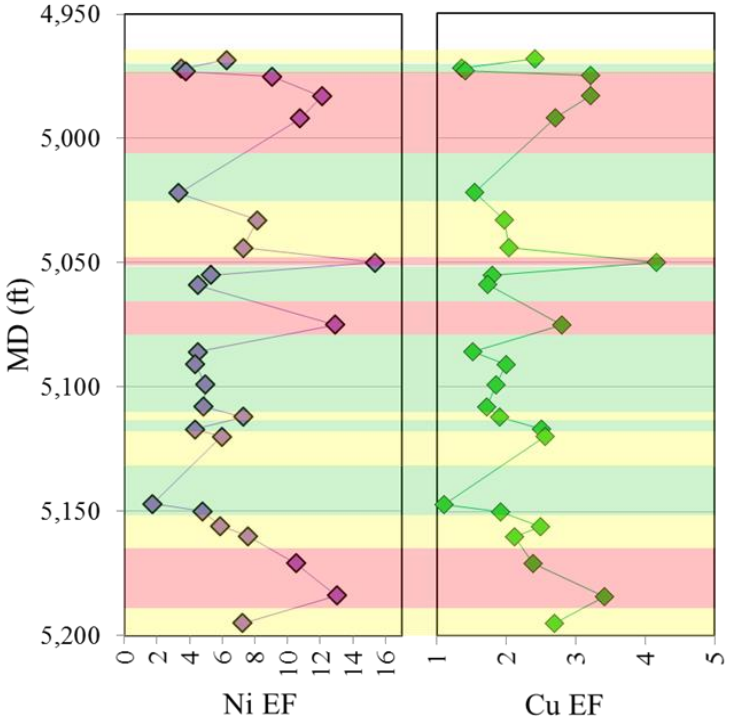

Figure 14: Ni and Cu EFs for the Mississippian Limestone core samples. Group 1 (Green) represents the lowest levels of productivity, Group 2 (Yellow) represents moderate levels of productivity and Group 3 (Red) represents high levels of productivity.

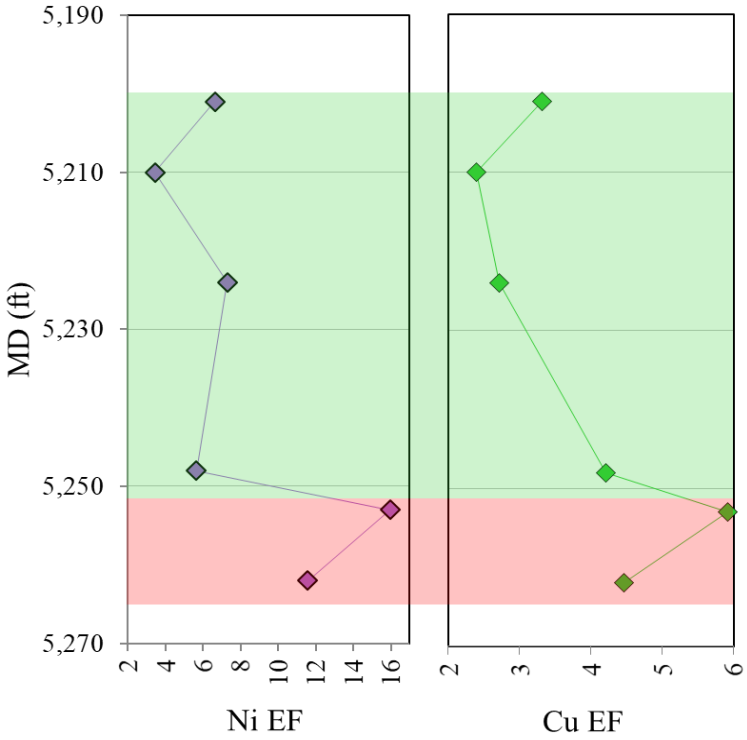

Figure 15: Ni and Cu EFs for the Woodford Shale core samples. Group 1 (Green) represents lower productivity during deposition and Group 2 (Red) represents higher productivity.

Within the Mississippian Limestone interval, Ni EFs range from 1.7 to 15.4 and Cu EFs range from 1.1 to 4.2. In attempting to divide the interval into smaller groups using Ni and Cu EFs, the greater number of samples required specific ranges of each elemental EF to be set. Using Ni and Cu EFs, the 27 Mississippian Limestone samples were divided into 3 groups, shown in Figure 14, which include: Group 1 (Green): samples 2, 3, 7, 11, 12, 14-17, 19, 21 and 22 (Ni EFs range: 1.7-5.5; Cu EFs range: 1.1-2.5), Group 2 (Yellow): samples 1, 8, 9, 18, 20, 23, 24 and 27 (Ni EFs range: 5.5-9.0; Cu EFs range: 1.9-2.7), and Group 3 (Red): samples 4, 5, 6, 10, 13, 25 and 26 (Ni EFs range: >9.0; Cu EFs range: >2.3). Based on these Ni and Cu EFs results, we suggest that the samples within group 3 were deposited during times of high primary productivity, while samples from group 2 were deposited during times of lesser, but still high, primary productivity, and samples from group 1 were likely deposited during times which were associated with the lowest levels of productivity.

Within the Woodford Shale interval, Ni EFs range from 3.5 to 15.9 and Cu EFs range from 2.4 to 5.9. Using Ni and Cu EFs, the 6 Woodford samples were divided into 2 groups, shown in Figure 15, which include: Group 1 (Green): samples 28-31 (Ni EFs range: 3.5-7.3; Cu EFs range: 2.4-4.2), and Group 2 (Red): samples 32 and 33 (Ni EFs range: 11.6-15.9 and Cu EFs range: 4.5-5.9). The greater values of Ni and Cu EFs, in Group 2, suggest a greater organic matter flux and more sulfate-reducing conditions than those in Group 1.

5.2.3c Comparison of U, V and Mo with Ni and Cu

Comparing the Woodford Shale and Mississippian Limestone U, V and Mo EF paleoredox interpretations to the paleoproductivity interpretations provided by the Ni and Cu EFs, we can attempt to regroup the samples based on paleoredox depositional conditions and the associations of these sedimentary redox levels to past levels of water-column primary

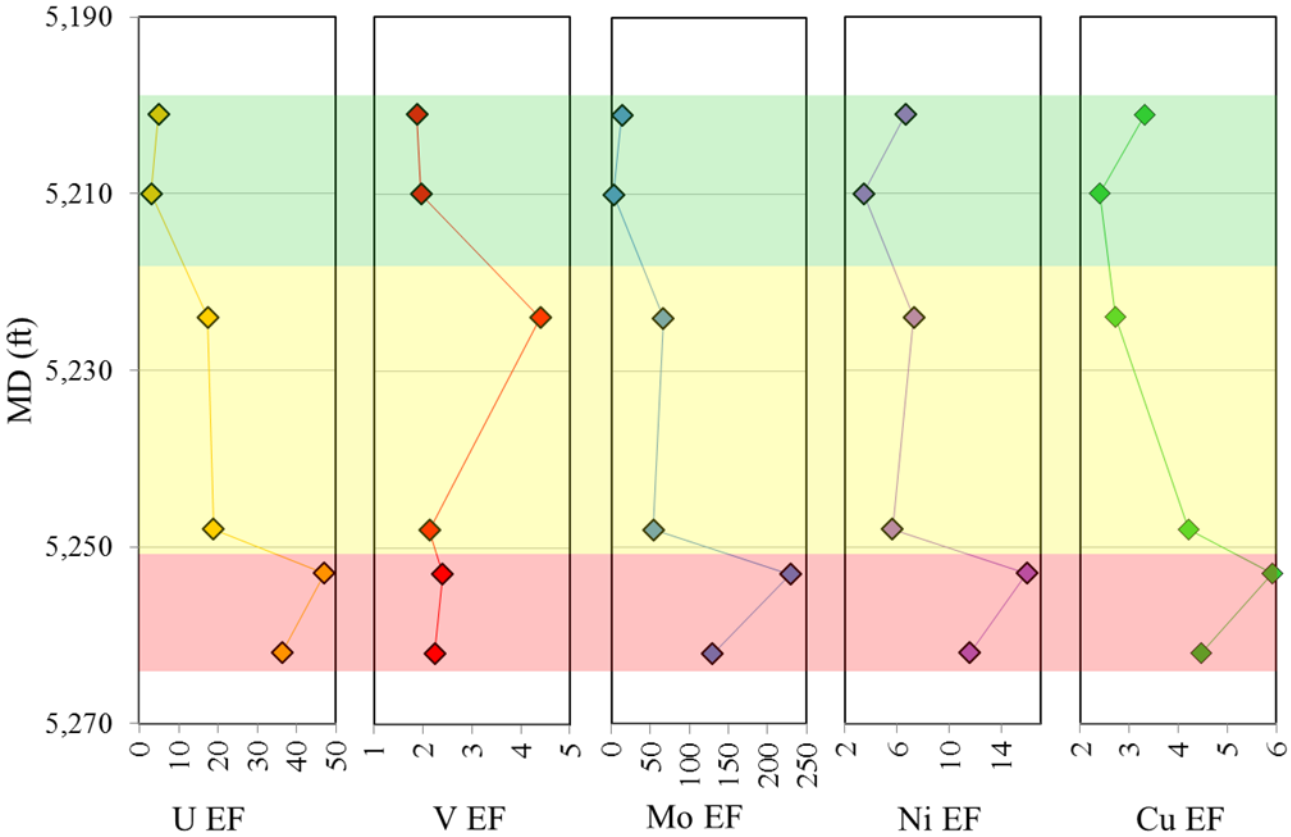

Figure 16: New groupings of the Woodford Shale core samples using U, V, Mo, Ni and Cu EFs. Group 1 (Green) represents suboxic-anoxic conditions with low productivity, Group 2 (Yellow) represents anoxic-euxinic conditions with low-moderate productivity and Group 3 (Red) represents anoxic-euxinic conditions with high productivity.

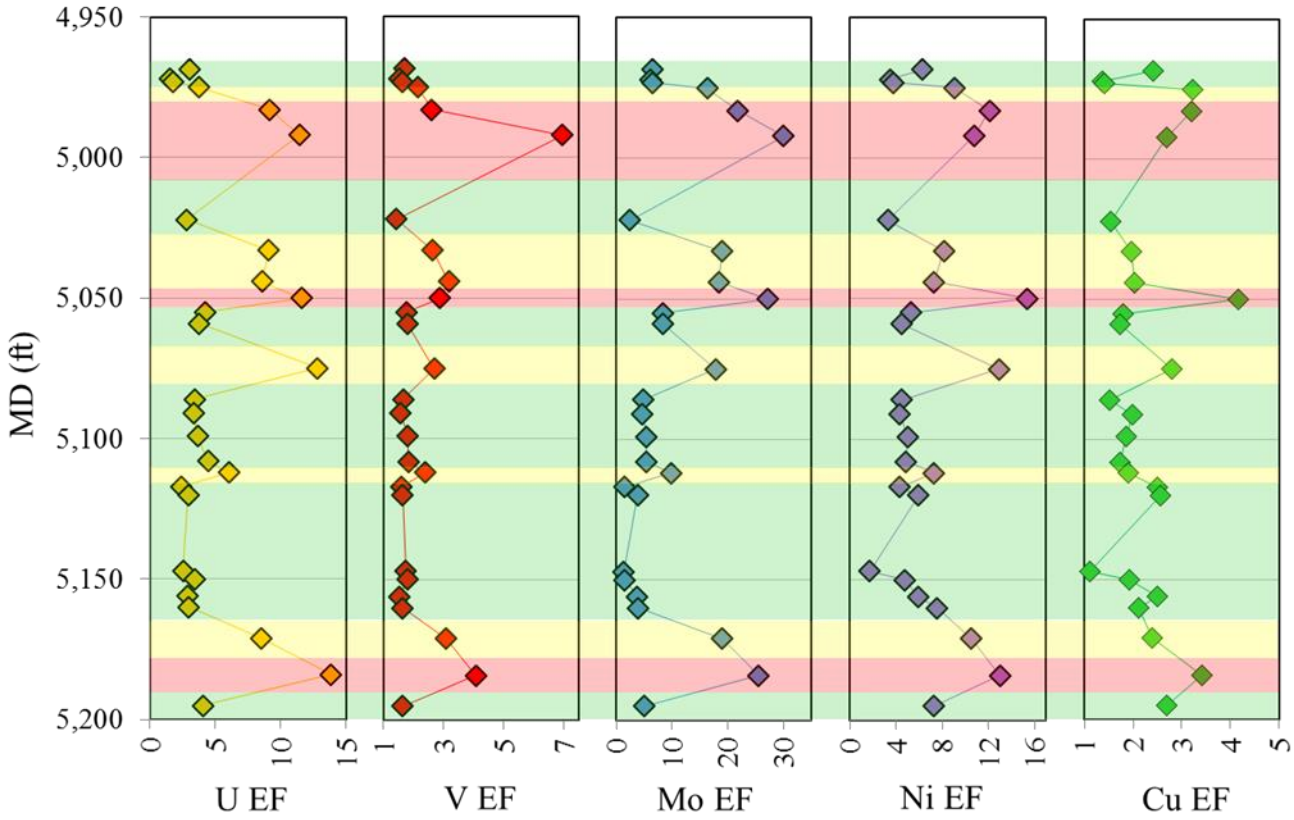

Figure 17: New groupings of the Mississippian Limestone core samples using U, V, Mo, Ni and Cu EFs. Group 1 (Green) represents suboxic-anoxic conditions with low productivity, Group 2 (Yellow) represents anoxic-euxinic conditions with low-moderate productivity and Group 3 (Red) represents anoxic-euxinic conditions with high productivity.

productivity. Figure 16 shows the Woodford Shale regrouping using U, V, Mo, Ni, and Cu EFs.

The new groups include: Group 1 (Green): samples 28 and 29 which were deposited in more suboxic-anoxic environments and are associated with low levels of primary productivity, Group 2 (Yellow): samples 30 and 31 were deposited in anoxic-possibly moderate euxinic environments and are associated with low-moderate levels of primary productivity and Group 3 (Red): samples 32 and 33 were deposited in anoxic-highly euxinic environments associated with high levels of primary productivity.

Figure 17 shows the Mississippian Limestone samples regrouped using the same classifications identified for the Woodford samples (green-yellow-red) using U, V, Mo, Ni and Cu EFs.

5.2.3d Covariation of Ni, Cu, Mo, U and V with TOC (wt. %)

Another useful method for interpreting paleoenvironments is to compare the trace element EFs with the total organic carbon content within the core samples. Tribovillard et al. (2006) (Figure 18) showed that the EFs of Ni, Cu, Mo, U and V were well correlated with TOC content. Tribovillard et al. (2006) explains that: 1) no matter what the redox conditions are, Ni-Cu EFs correlate positively with TOC content, except when dealing with very low TOC values, 2) U and V show good correlations with TOC values above and below certain thresholds and 3) above the threshold used in the U-V and TOC correlations, Mo enrichment is observed, suggesting the development of euxinic conditions where TOC values no longer correlate as well with U and V. Oxic-suboxic conditions are usually only observed when TOC is generally less than 2.0 wt.% and trace elements are deposited in association with the detrital fraction of the sediment. Anoxic but non-sulfidic conditions are observed when variable TOC values correlate

well with trace element EFs, and euxinic conditions, in which free H_2S is present, are observed when strong U and V enrichments and weak correlations with TOC are present. Tribovillard et al. (2006) explain that elements such as V and U can be reduced and can accumulate under denitrifying conditions, whereas other elements such as Ni, Co, Cu and Mo are enriched mainly under sulfate-reducing conditions.

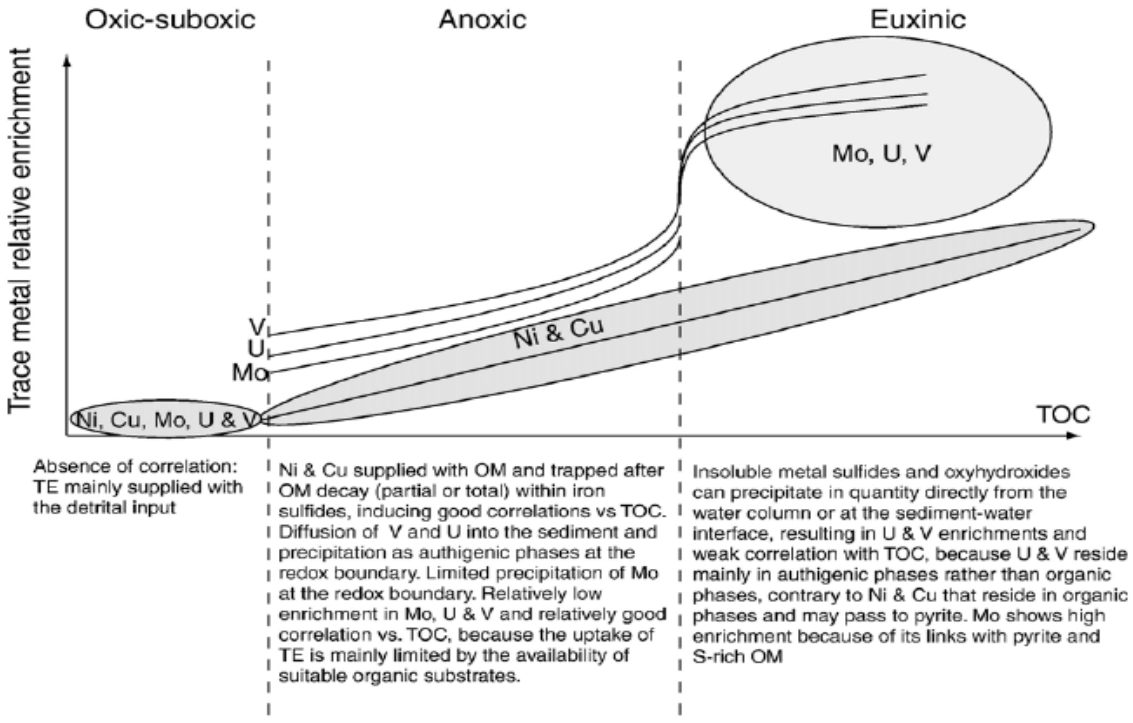

Figure 18: Diagram illustrating the relative enrichment of Ni, Cu, Mo, U and V vs. TOC, adapted from Tribovillard et al. (2006). TE stands for trace elements and OM stands for organic matter.

We plotted TOC wt.% versus our trace metal EFs in Figures 19 (U), 20 (V), 21 (Mo), 22 (Ni) and 23 (Cu). In all of these figures, the Woodford Shale samples are shown in orange squares while the Mississippian Limestone samples are shown in blue circles. Several of the trace element EFs yield positive correlations with TOC. In Figures 19 and 21 there are two distinct trends, one for the Woodford Shale samples and one for the Mississippian Limestone samples, each having a significant positive correlation (see r^2 correlation coefficient in Figures 19 and 21) between U (or Mo) EFs and TOC. The variability between V EF and TOC (Figure 20) is not as straightforward but may be explained by the complex redox-characteristics of V. Jones and Manning (1994) explain that V may be bound to organic matter by the incorporation of V^{4+} into porphyrins, and is concentrated in sediments deposited under reducing conditions (Shaw et al., 1990; Emerson and Huested, 1991). However, it is not always correlated with organic matter, and may be physically hosted by detrital silicate minerals (Glikson et al., 1985; Stow and Atkin, 1987; Jones and Manning, 1994). This could very well explain the poor correlation between V enrichment and TOC content in the samples.

Figures 22 and 23 show the TOC vs. Ni EF and TOC vs. Cu EFs, respectively. There are significant positive correlations (see r^2 correlation coefficients in Figures 22 and 23) between Ni (or Cu) EFs and TOC, for both units. As suggested by Tribovillard et al. (2006) it is likely that these trace elements correlate well with TOC, regardless of redox conditions.

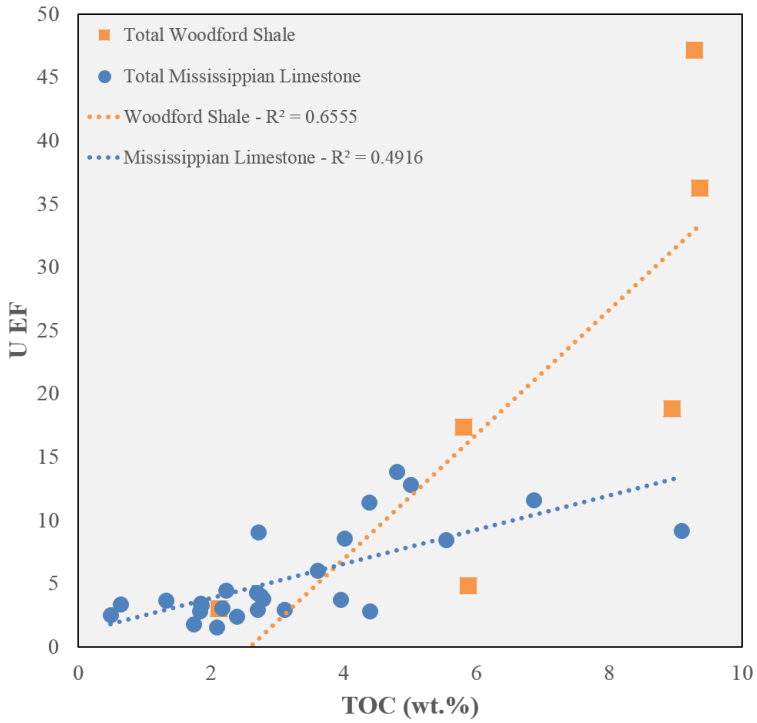

Figure 19: TOC wt.% vs. U EF for Woodford Shale core samples (orange squares) and Mississippian Limestone core samples (blue circles).

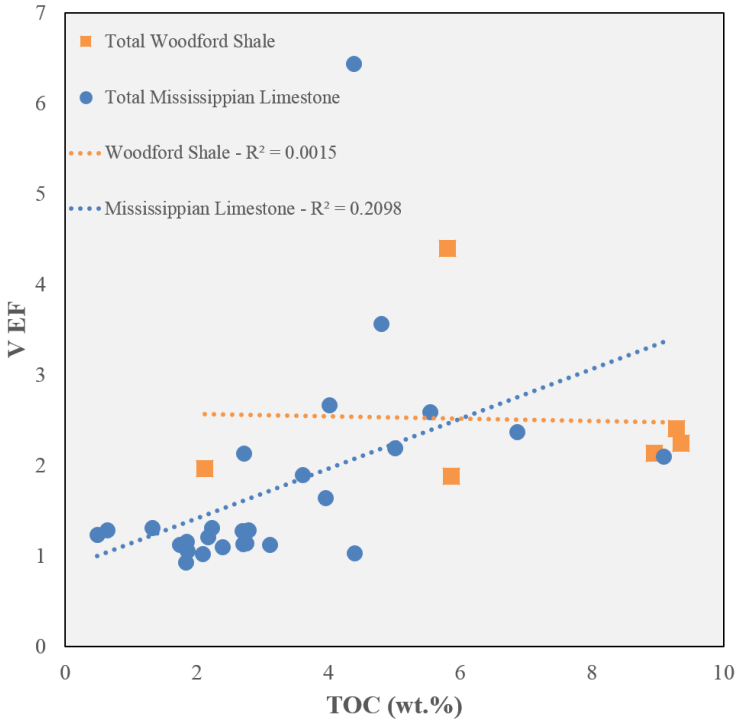

Figure 20: TOC wt.% vs. V EF for Woodford Shale core samples (orange squares) and Mississippian Limestone core samples (blue circles).

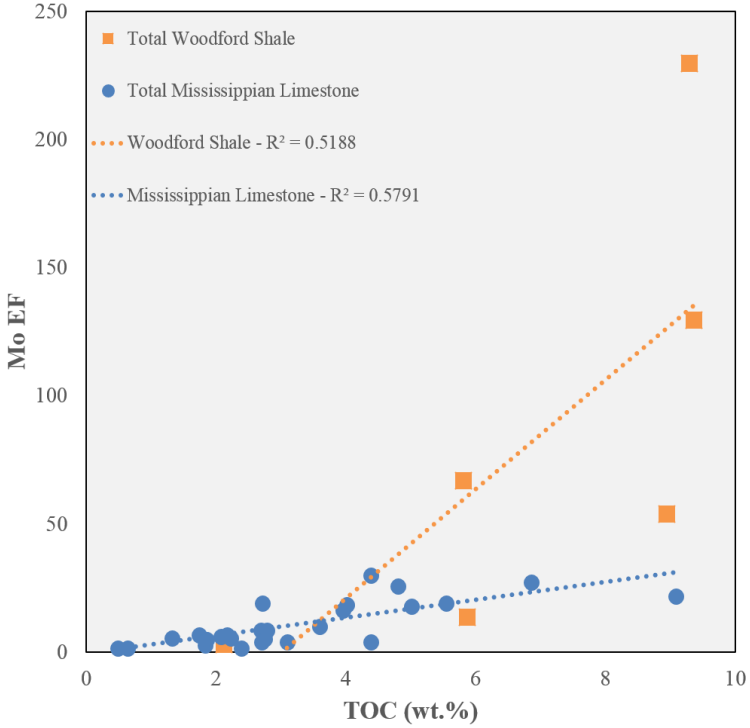

Figure 21: TOC wt.% vs. Mo EF for Woodford Shale core samples (orange squares) and Mississippian Limestone core samples (blue circles).

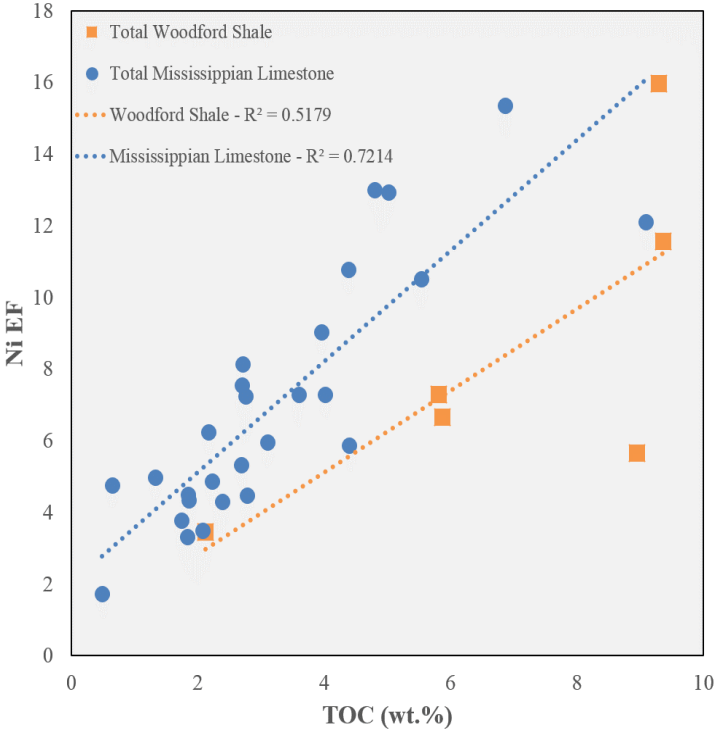

Figure 22: TOC wt.% vs. Ni EF for Woodford Shale core samples (orange squares) and Mississippian Limestone core samples (blue circles).

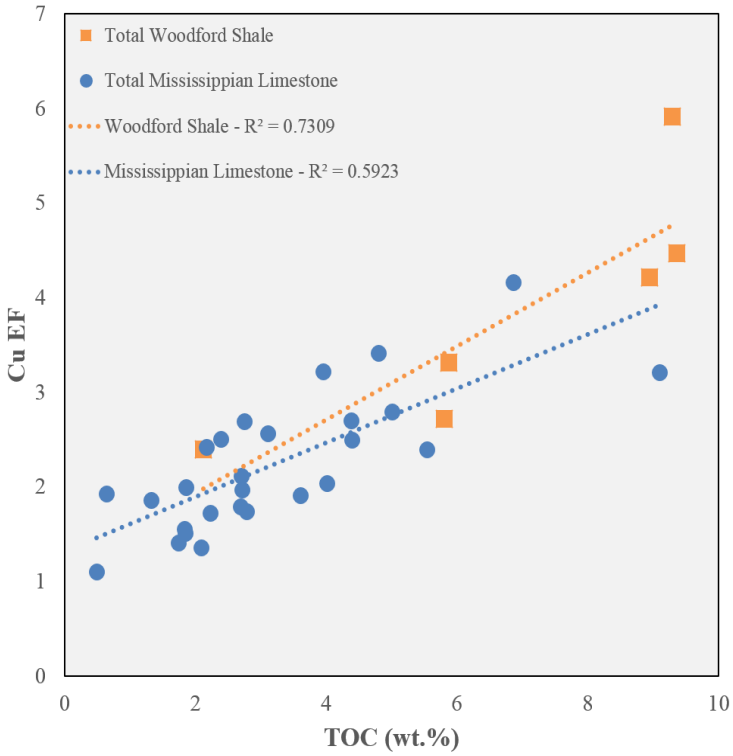

Figure 23: TOC wt.% vs. Cu EF for Woodford Shale core samples (orange squares) and Mississippian Limestone core samples (blue circles).

We attempt to corroborate our previously identified paleoredox depositional divisions (Groups 1, 2 suboxic-anoxic and Group 3 euxinic) using our trace metal enrichment factor data for the Mississippian Limestone core samples, for which significantly more data (compared to the Woodford samples) exist. In figures 24-28, we color code the data from the samples previously identified as having been deposited under suboxic-anoxic conditions as red, and those identified as having being deposited under euxinic conditions as green.

Figures 24, 25 and 26 show U EF, V EF and Mo EF vs. TOC wt.%, respectively, for the Mississippian Limestone core samples. Remarkably, our previously-determined paleoredox

anoxic-euxinic grouping also shows a clear demarcation in the anoxic-euxinic boundary that is consistent with a TOC value of about 5 wt.%. Although the trends in figures 24-26 are weak, there is a clear break in the data at about 5% between the anoxic and euxinic samples. Even more remarkable are the consistent and statistically significant correlations across all groupings (i.e., anoxic and euxinic) when plotting Ni and Cu EFs vs. TOC wt.% (Figures 27 and 28). This is identical to and, therefore, strongly supports the schematic model first proposed by Tribovillard et al. (2006). Our data, however, adds numbers (specifically the break in TOC wt.% at 5%) to the schematic model and suggests sulfur-replete conditions at TOC wt.% values of 5% or more.

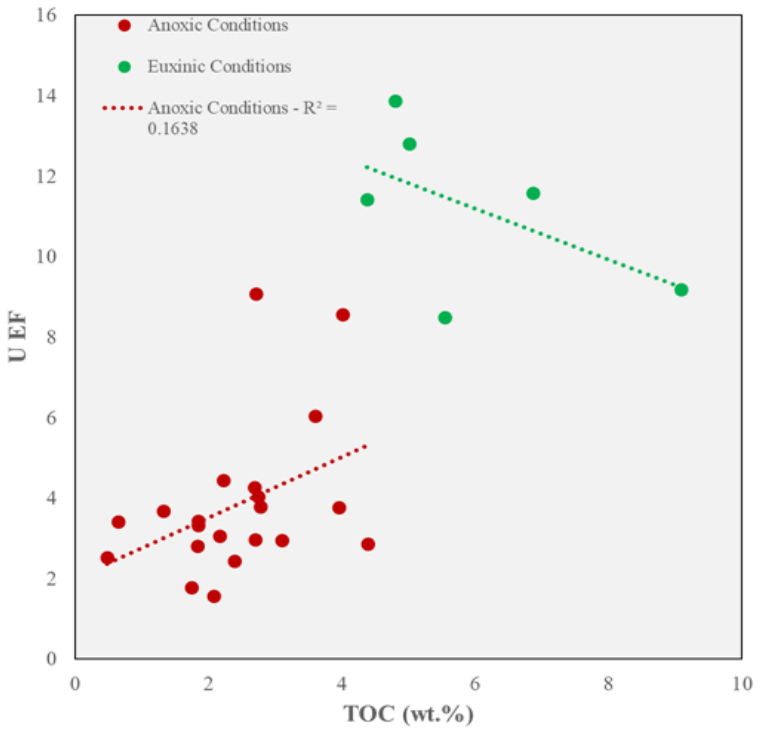

Figure 24: TOC wt.% vs. U EF for Mississippian Limestone core samples using the classification scheme from Tribovillard et al. (2006). The red circles represent anoxic conditions and the green circles represents euxinic conditions. The red and green trend lines represent the correlation between TOC and the EF for anoxic and euxinic conditions, respectively.

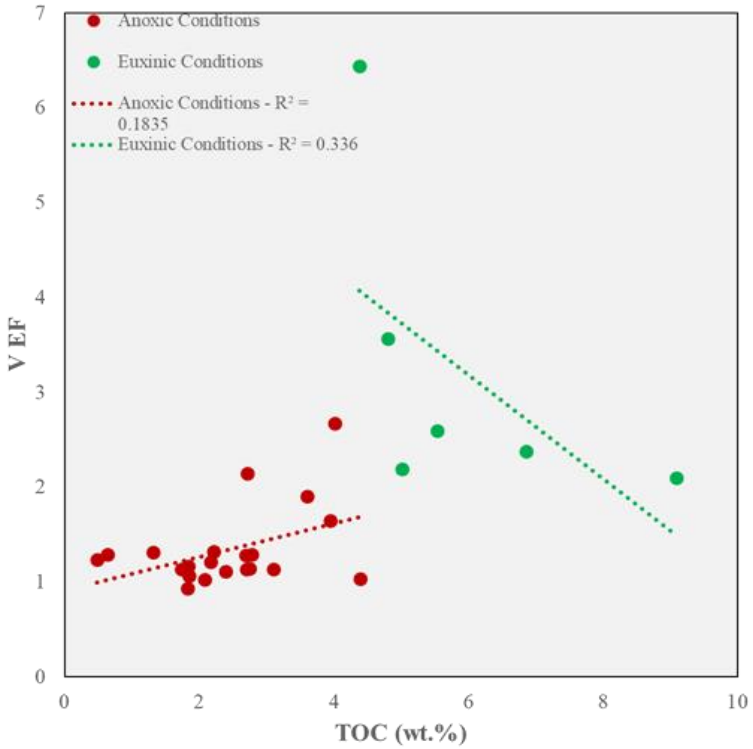

Figure 25: TOC wt.% vs. V EF for Mississippian Limestone core samples using the classification scheme from Tribovillard et al. (2006). The red circles represent anoxic conditions and the green circles represents euxinic conditions. The red and green trend lines represent the correlation between TOC and the EF for anoxic and euxinic conditions, respectively.

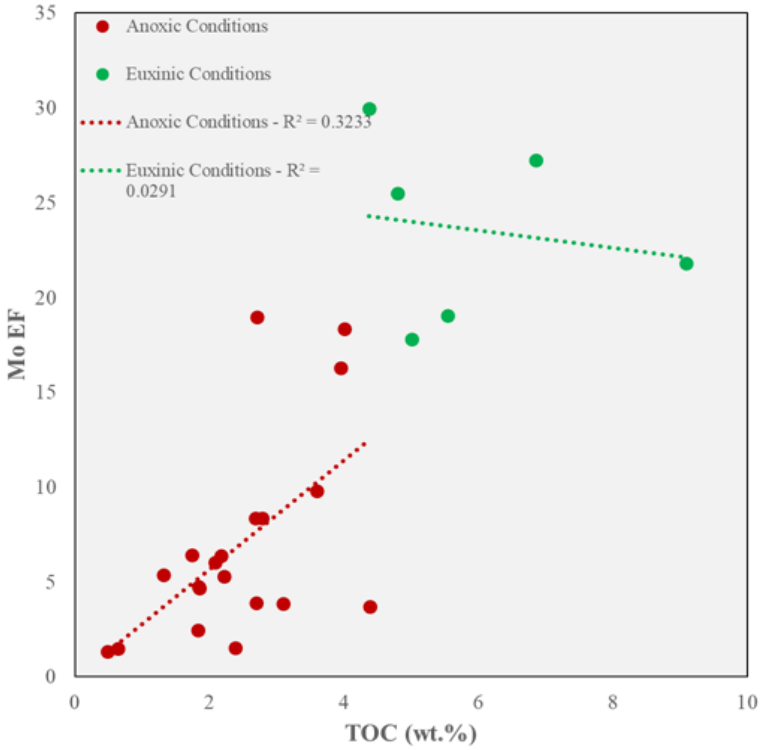

Figure 26: TOC wt.% vs. Mo EF for Mississippian Limestone core samples using the classification scheme from Tribovillard et al. (2006). The red circles represent anoxic conditions and the green circles represents euxinic conditions. The red and green trend lines represent the correlation between TOC and the EF for anoxic and euxinic conditions, respectively.

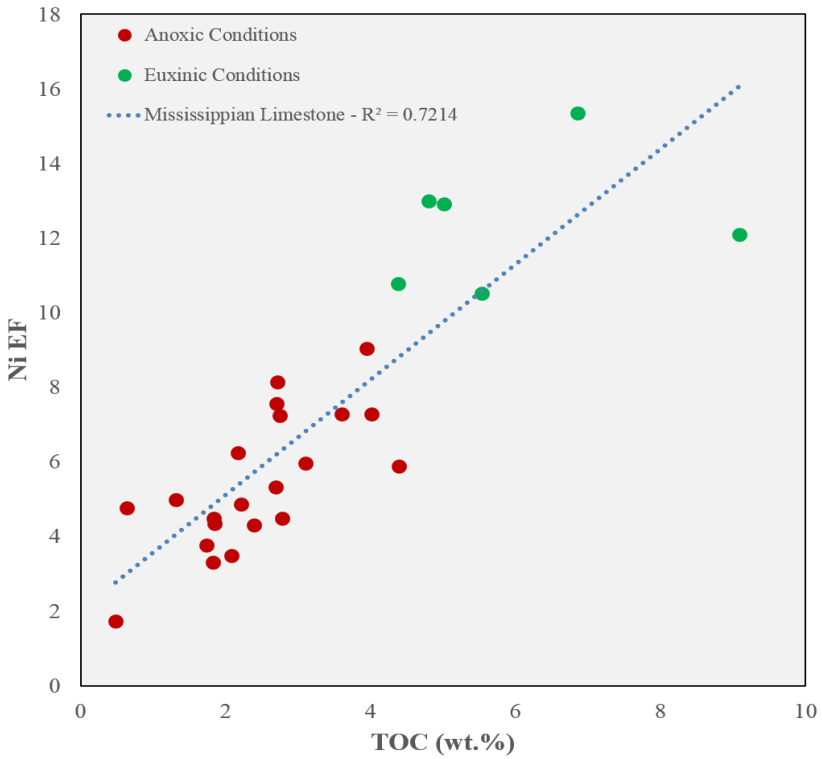

Figure 27: TOC wt.% vs. Ni EF for Mississippian Limestone core samples using the classification scheme from Tribovillard et al. (2006). The red circles represent anoxic conditions and the green circles represents euxinic conditions. The red and green trend lines represent the correlation between TOC and the EF for anoxic and euxinic conditions, respectively.

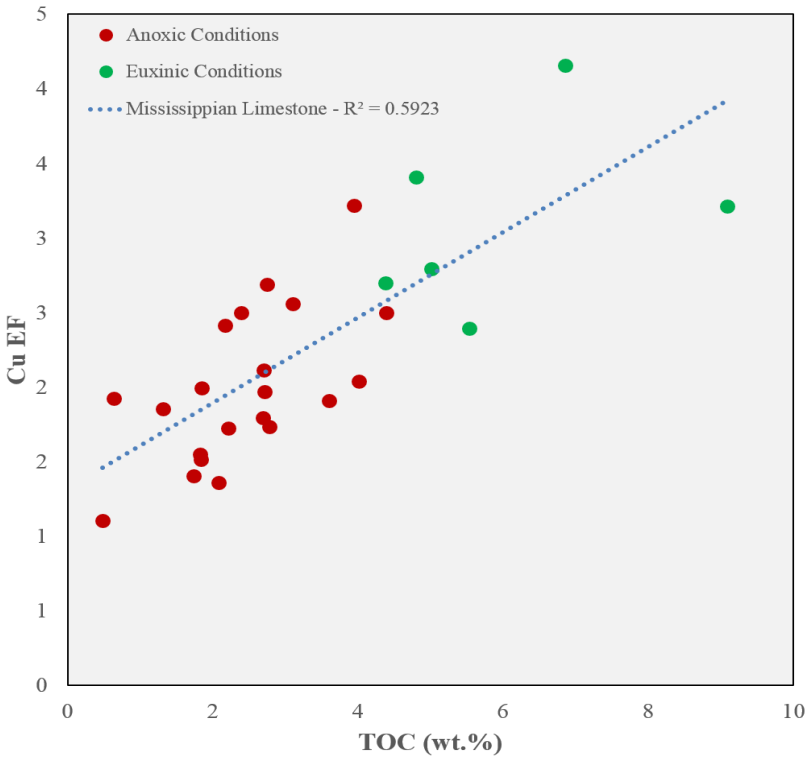

Figure 28: TOC wt.% vs. Cu EF for Mississippian Limestone core samples using the classification scheme from Tribovillard et al. (2006). The red circles represent anoxic conditions and the green circles represents euxinic conditions. The red and green trend lines represent the correlation between TOC and the EF for anoxic and euxinic conditions, respectively.

5.3 Oil Sample Analysis

Previous studies (Akinlua et al., 2007a; Curiale, 1987; Barwise, 1990; Udo et al., 1992; Oluwole et al., 1993; Nwachukwu et al., 1995) have indicated that transition metals can be used as reliable parameters for crude oil characterization and oil-oil and oil-source rock correlations. Trace metals are incorporated into oils in the form of porphyrin complexes in petroleum source rocks and may include direct incorporation from the biomass and formation during sedimentation (Akinlua et al., 2007a). Akinlua et al. (2007a) explain that the nature of occurrence of metals, their distribution patterns and concentrations in crude oils can give information on the origin, depositional environment and migration of petroleum (Ellrich et al., 1985; Barwise, 1990; Oluwole et al., 1993).

We were able to follow the same organic matter interpretation method that we used for the core samples. However, due to the lack of sulfur data and being unable to calculate EFs for the oil samples, we could not repeat the same paleoredox and depositional environment interpretation methods. EFs could not be calculated for the oil samples because, as stated earlier, no reference material exists for the oils and the trace element concentrations within oils change during in-reservoir alteration events. For these reasons, we followed a number of previous studies performed on oils and source rocks which will be discussed in the following sections.

Lewan (1984), Barwise (1990), Udo et al. (1992) and Akinlua et al. (2007a) explain that the ratios of transition metals in crude oil are useful in the determination of source rock type and depositional environment because they remain unchanged irrespective of diagenetic and in-reservoir alteration effects. In order to determine the organic matter type and depositional environments of the oil sample's origins, we used trace elemental ratios determined from our

HR-ICP-MS analysis. The trace elemental ratios of interest include V/Ni and Co/Ni. The ratios for the oil samples are shown in Table 5.

5.3.1 Organic Matter Classification in Oil Samples

Since source rock organic matter is the direct precursor of petroleum, it is expected that the trace metal contents of organic matter should be reflective of those in the oil (Akinlua et al., 2007b). It has been shown by Lewan (1984), Barwise (1990), Barwise (1992), Udo et al., (1992), Akinlua et al. (2007a), Galarraga et al. (2008), Mudiaga (2011) and Lopez and Lo Monaco (2017) that marine organic matter typically has high Ni and V concentrations (high V/Ni ratios; >3) because marine source rocks are deposited with an abundant input of porphyrin-precursor chlorophylls to the organic matter. Lacustrine source rocks typically contain a moderate quantity of Ni and V (moderate V/Ni ratios; 1.9-3) and terrestrially-derived source rocks contain small amounts of Ni and V (low V/Ni ratios; <1.9) (Akinlua et al., 2007a; Barwise, 1992; Barwise, 1990). This is because of the lack of porphyrin-precursor chlorophylls within the organic matter.

Figure 29 shows V vs. Ni for the crude oil samples from the Anadarko basin. The V/Ni ratios for these oils range from 0.12-3.02. From this figure, we can see a clear distinction between two groups of oils: Group A contains samples WO5 (V/Ni of 3.02) and WO6 (V/Ni of 2.68) and Group B contains samples WW (V/Ni of 0.41), PW (V/Ni of 0.7), MW (V/Ni of 0.12), WO1 (V/Ni of 0.79), WO2 (V/Ni of 0.75) and WO3 (V/Ni of 0.22). This indicates that the samples in Group A were derived from predominantly marine or mixed marine and terrigenous organic matter and the samples in Group B were derived from predominantly terrigenous organic matter.

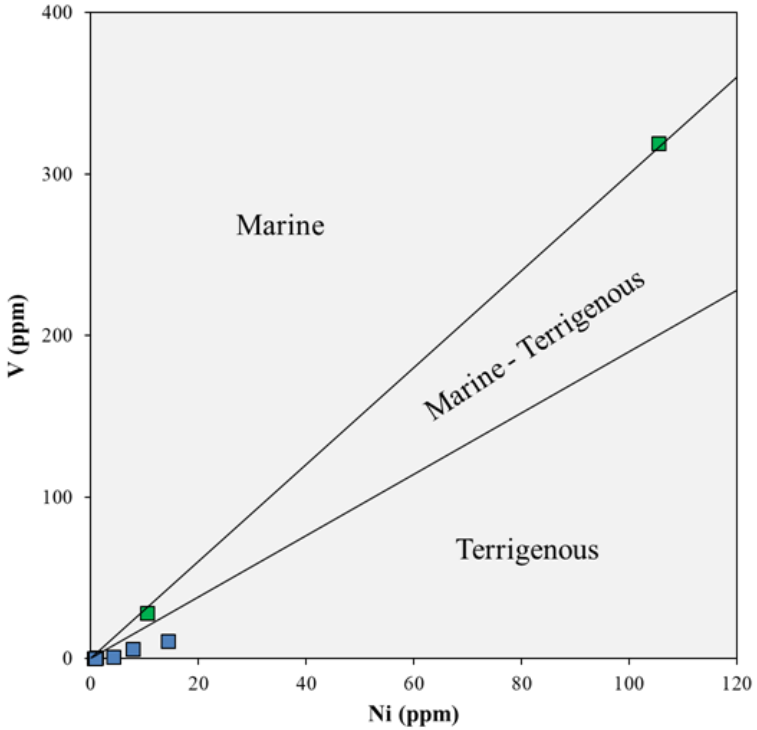

Figure 29: Ni vs. V for the oil samples (modified from Galarraga et al., 2008). Group A samples represented by green squares and Group B samples represented by blue squares.

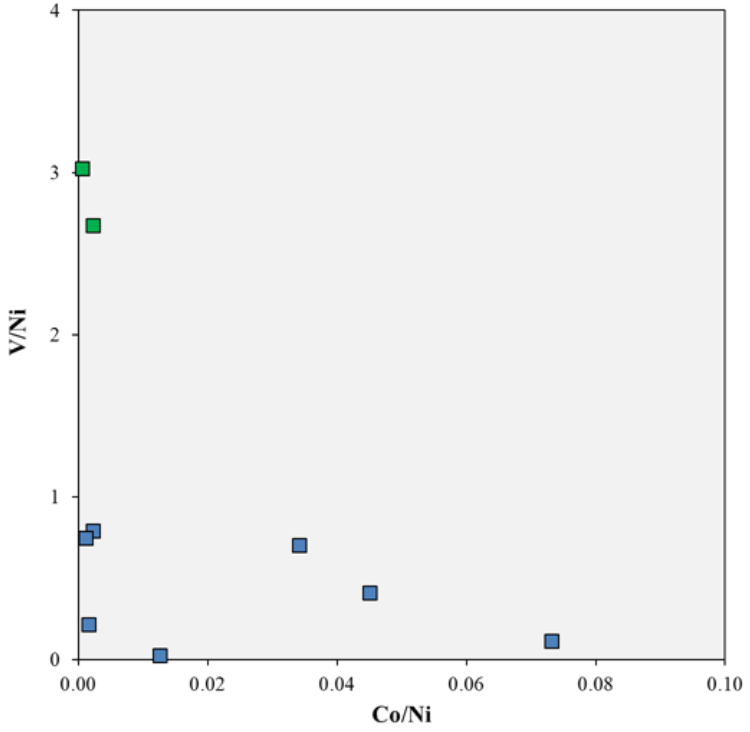

Figure 30: Co/Ni vs. V/Ni for the oil samples. Group A samples represented by green squares and Group B samples represented by blue squares.

5.3.2 Paleoredox Determination in Oil Samples

Lewan and Maynard (1982), Lewan (1984), Barwise (1990), Udo et al. (1992), Akinlua et al. (2007a) and Akinlua et al. (2016) explain that source rock depositional environment determines the proportion of V to Ni in crude oils. Enriched V content compared to Ni in source rocks occurs in anoxic environments (Peters and Molowan, 1993; Akinlua et al., 2016). Lewan and Maynard (1982), Lewan (1984), Barwise (1990), Udo et al. (1992), Akinlua et al. (2007a), Galarraga et al. (2008) and Akinlua et al. (2016) show that high V/Ni ratios are associated with anoxic paleoenvironment of deposition. Both high V/Ni and Co/Ni ratios indicate anoxic/oxic depositional environments and low values of V/Ni ratios indicate deposition under oxic conditions. Figures 29 and 30 show V vs/ Ni and V/Ni vs. Co/Ni, respectively, for the Anadarko Basin oil samples. There are two distinct groups: Group A (green squares) and Group B (blue squares). These figures show that Group A samples contain high V/Ni values and low Co/Ni values, indicating that the corresponding source rocks for these samples were deposited in anoxic conditions. Group B samples contain low V/Ni values and low-moderate Co/Ni values, indicating that the corresponding source rocks for these samples were deposited in oxic-suboxic conditions.

5.4 Classification and Correlation

Prior studies (Curiale, 1987; Hirner, 1987; Barwise, 1990; Udo et al., 1992; Oluwole et al., 1993; Filby, 1994; Nwachukwu et al., 1995; Akinlua et al., 2007a; Akinlua et al., 2015) have indicated that biologically important elements such as V, Ni and Co can be used as reliable parameters for oil-oil and oil-source correlations (Gao et al., 2015). Trace element concentrations can be influenced by in-reservoir alteration processes such as thermal degradation and biodegradation as well as migration (Al-Shahristani and Al-Atyia, 1972; Tissot and Welte, 1984;

Barwise, 1990; Greibokk et al., 1994; Lopez et al., 1995). However, trace element ratios of crude oils are often constant and have been widely used in correlation studies (Gao et al., 2015; Hirner, 1987; Akinlua et al., 2007a; Akinlua et al., 2015; Shi et al., 2015). Oil and organic matter studies such as those completed by Akinlua et al. (2007a), Akinlua et al. (2010), and Akinlua et al. (2016) show that there are significant and positive correlations between Co and V with Ni, suggesting that these ratios can be used as oil classification or correlation tools. The ratios used in this study include V/Ni and Co/Ni.

5.4.1 Oil-Oil Correlations

Oil-oil correlations are important and valuable tools that can be extremely useful in petroleum exploration. This tool enables oils discovered in a basin to be grouped according either to a common source or to a common organic matter type (Barwise, 1990). Being able to determine a common source of the discovered oil could have the potential to reveal undiscovered oil fields and information about the basin that could help in large scale modeling projects. Using the organic matter type and depositional environment interpretations from the previous sections, we are able to group the oils in this study.

In the previous sections, we were able to determine two main groups for the oil samples by using the V/Ni and Co/Ni ratios. Figures 29 and 30 show that these two groups show nearly opposite trends for the ratios studied here. Group A includes samples WO5 (Woods Co.; V/Ni of 3.02; Co/Ni of 0.002) and WO6 (Alfalfa Co.; V/Ni of 2.68; Co/Ni of 0.016). Group B contains samples WW (Logan Co.; V/Ni of 0.41; Co/Ni of 0.072), PW (Payne Co.; V/Ni of 0.7; Co/Ni of 0.03), MW (Logan Co.; V/Ni of 0.12; Co/Ni of 0.06), WO1 (Lincoln Co.; V/Ni of 0.79; Co/Ni of 0.007), WO2 (Lincoln Co.; V/Ni of 0.75; Co/Ni of 0.003) and WO3 (Lincoln Co.; V/Ni of 0.22; Co/Ni of 0.006).

From these results, we can interpret that Group A samples were generated from source rocks that contained predominantly marine organic matter and were deposited under anoxic-possibly euxinic conditions. For the Group B samples, we can interpret that the oils were generated from source rocks that contained predominantly terrigenous organic matter and were deposited under more suboxic conditions.

One important thing to note, however, is the location of which the oils were sampled. Group A samples were produced from Woods and Alfalfa Counties and, by referring back to Figure 1, we can see that these counties are located in the western portion of the study area (west of the Nemaha uplift). Group B samples were produced from Logan, Payne and Lincoln Counties which are located on the eastern side of the study area (east of the Nemaha uplift). Being able to group the samples, not only by trace elements, but also by location, provides us with confidence that our oil-oil correlations are accurate.

5.4.2 Oil-Source Rock Correlations

By analyzing, comparing and interpreting the trace element concentrations and ratios of in source rocks and produced crude oils, oil-source rock correlations can be made, allowing for better interpretations of oil migration pathways and accumulation characteristics. Filby (1994), Akinlua et al. (2007a), Jiao et al. (2010) and Lopez and Lo Monaco (2017) explain that V and Ni are the most abundant trace metals in crude oils, bitumen and kerogen, and their association with organic matter depends on factors related to diagenesis. A study performed by Akinlua et al. (2007b) showed that Ni and V enrichment occurs in the oils relative to the source rock. Higher enrichment in oils, relative to kerogens in source rocks, could be a consequence of uptake of these metals, during oil migration, when the oil comes into contact with interstitial waters

(Akinlua et al., 2007b; Lewan and Maynard, 1982). Therefore, using V and Ni for oil-source rock correlations could allow for oil migration to be better tracked throughout the basin.

In attempting to correlate the oil samples with the source rocks in this study, we used the results of the methods previously discussed for organic matter and paleoredox interpretations. Figures 31 and 32 show V vs. Ni and Co/Ni vs. V/Ni, respectively, for the core and oil samples. In Figure 31 (V vs. Ni), we can see that Group B oil samples show the same trend as the Mississippian Limestone samples and possibly 2 of the Woodford Shale samples. The Woodford Shale samples, overall, do not show a significant trend and the Group A oil samples do not correlate well with any of the core samples, as they contain V/Ni values close to 3. In Figure 32 (Co/Ni vs. V/Ni), we see that there are two distinct trends, one for the Woodford Shale and the other for the Mississippian Limestone samples. However, we recall here that the Woodford Shale samples appeared to show multiple paleoredox conditions (section 5.2). Hence, we can say that this trend in Figure 32 does not represent the Woodford Shale as a whole. The Group A oil samples in Figure 32 do not correlate to the core samples. However, the Group B oil samples appear to have similar Co/Ni and V/Ni values to those of the Mississippian Limestone and 3 of the Woodford Shale core samples. The other 3 Woodford Shale samples do not appear to correlate with any of the oil samples.

In using trace element ratios for oil-source rock correlations, we were able to interpret that the Group B oil samples follow a similar trend to that of the Mississippian Limestone core samples and 3 of the Woodford Shale samples. The Group A oil samples and other 3 Woodford Shale core samples, however, do not show any types of correlations. There could be a number of reasons, or combination of reasons, that explain why these correlations are not present, including: 1) the Group A oils were actually generated from source rocks other than the

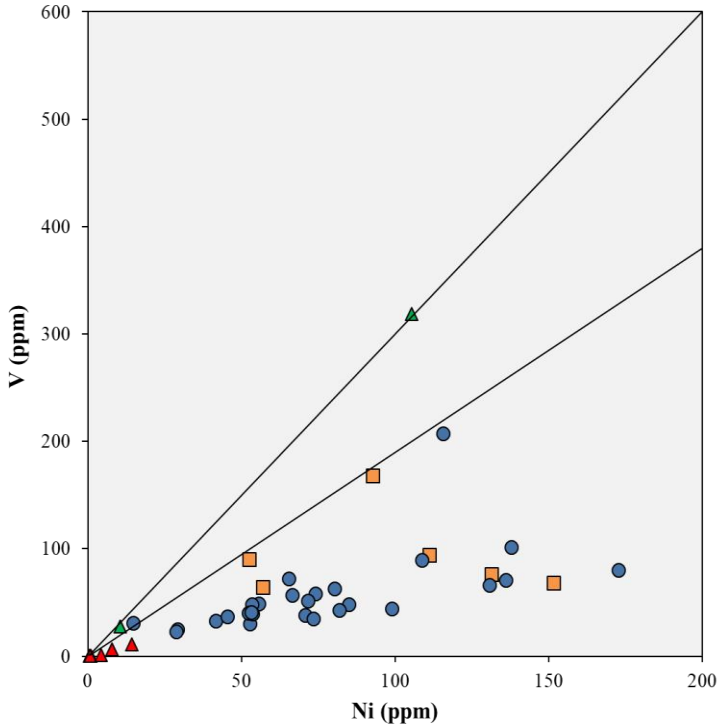

Figure 31: V vs. Ni for Woodford Shale core samples, Mississippian Limestone core samples and the oil samples. The orange squares represent the Woodford Shale core samples, the blue circles represent the Mississippian Limestone core samples, the green triangles represent the Group A oil samples and the red triangle represent the Group B oil samples. The black lines represent the thresholds of 1.9 and 3 for V/Ni ratio.

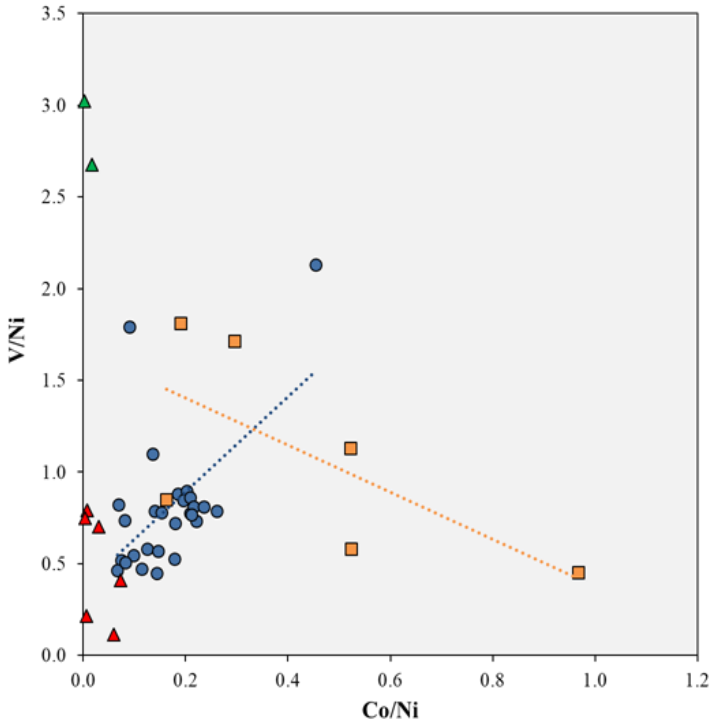

Figure 32: V/Ni vs. Co/Ni for Woodford Shale core samples, Mississippian Limestone core samples and the oil samples. The orange squares represent the Woodford Shale core samples, the blue circles represent the Mississippian Limestone core samples, the green triangles represent the Group A oil samples and the red triangle represent the Group B oil samples. The orange and blue trend lines represent the Woodford Shale and Mississippian Limestone core sample trends, respectively.

Woodford Shale or Mississippian Limestone, 2) the fact that we measured trace metals in whole rock rather than in extracted bitumen or kerogen, and trace elements are known to be more concentrated in the bitumen and kerogen, or 3) the oils were generated from the source rocks studied here, but they were generated at a location in the basin that underwent much different depositional settings than that of the studied core samples (i.e. shelf vs. deep basin). This could very well be the case for the Group A oil samples since we can see a much higher V and Ni content in these oils than in the Group B oils or the core samples. This enrichment in V and Ni suggests that these oils were generated from marine organic matter, indicating the oils could have been produced in the deep portion of the basin and migrated up-dip to the Anadarko Shelf region where they were produced. In order for us to accurately make this interpretation, we would need to compare a larger number of samples (core and oil) from a larger sampling area (across the entire basin; shelf and deep basin).

5.5 Depositional Profile

We used multiple paleoredox methodologies and proxies to ultimately determine the most accurate profile of deposition for the Woodford Shale and Mississippian Limestone core samples. For these rock samples, we determined 1) the organic matter input by using the trace element ratios of V/Ni, V/Ni vs. Co/Ni and Co/Ni vs Mo/Ni and 2) the paleoredox conditions during deposition using the V/(V+Ni) ratio and S content, and the U, V, Mo, Ni and Cu EFs and TOC content. From the results of these analyses, we interpret that: 1) there was a predominantly terrigenous organic matter source to the Woodford Shale and the Mississippian Limestone during deposition at this location, 2) the Woodford Shale and Mississippian Limestone samples were deposited under 3 different paleoredox conditions including: suboxic-anoxic conditions with low productivity, anoxic-euxinic conditions with low-moderate productivity and anoxic-euxinic

conditions with high productivity, and 3) the TOC content threshold between anoxic and euxinic conditions, for the Mississippian Limestone samples, occurs at ~5 wt.% TOC. With these interpretations, we were then able to create depositional profiles for the samples. Zone 1 is characterized by suboxic-anoxic conditions with low productivity and predominantly terrigenous organic matter input, Zone 2 is characterized by anoxic-euxinic conditions with low-moderate productivity and predominantly terrigenous organic matter input and Zone 3 is characterized by anoxic-euxinic conditions with high productivity and predominantly terrigenous organic matter input. We then plotted these zones vs. depth (Figure 33) (Kelly, 2016) and were able to accurately create a schematic model (Figure 34 and 35) showing the depositional profile of the Woodford Shale and Mississippian Limestone units in this location. Figure 33 may be an oversimplification of the depositional profiles of these two units, but it adequately illustrates the depositional and paleoredox conditions for the Woodford Shale and Mississippian Limestone.

Zone 1 exists within the upper portion of the Woodford Shale and multiple times throughout the Mississippian Limestone. These suboxic-anoxic conditions with low-moderate productivity occurred during periods of lower sea-levels which are usually marked by low-moderate organic matter preservation and low-moderate trace metal enrichment (Tribovillard et al., 2006). The low-moderate Ni and Cu content, combined with the low-moderate V, Mo and TOC content, suggests that there were low levels of primary productivity and the water column was mostly oxygen-rich, only allowing for low-moderate amounts of the terrigenous organic matter to reach the sediments and be preserved. The low-moderate TOC content in Zone 1 for the Woodford Shale and Mississippian Limestone units range from 2.12-5.87 wt.% and 0.48-4.39 wt.%, respectively, further supporting this interpretation. In this zone, the Woodford Shale

samples contain a high TOC content, suggesting a greater terrigenous organic matter influx during this time.

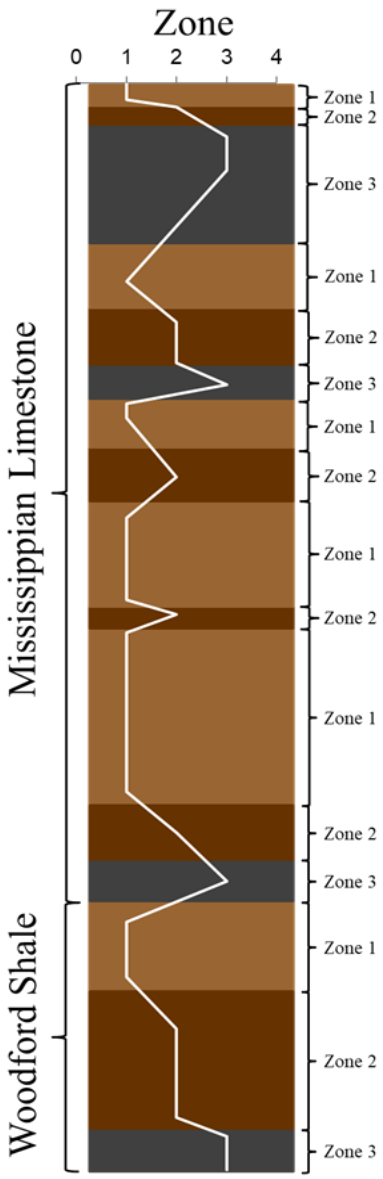

Figure 33: Depositional Profile for the Woodford Shale and Mississippian Limestone.

Zone 2 exists within the middle portion of the Woodford Shale and multiple times throughout the Mississippian Limestone. These anoxic-euxinic conditions with low-moderate productivity occurred during periods of higher sea-levels (i.e., greater water depths) which can be marked by moderate to high organic matter preservation and moderate-high metal enrichment (Tribovillard et al., 2006). The low-moderate Ni and Cu content, combined with the moderate-high V, Mo and TOC content, suggests that there were low-moderate levels of primary productivity and the water column was less oxygen-rich, allowing a greater amount of organic matter to reach the sea floor and be preserved in the sediment. The TOC contents in Zone 2 for the Woodford Shale and Mississippian Limestone units range from 5.81-8.95 wt.% and 2.71-5.54 wt.%, respectively, further supporting this interpretation. The increased amounts of TOC content in the Woodford Shale suggests that, during this time, a greater influx of terrigenous organic matter was being supplied to the sediments.

Zone 3 exists within the lower portion of the Woodford Shale and only a few times throughout the Mississippian Limestone. These anoxic-euxinic conditions with high productivity occurred during periods of increased sea-level (greater water depths) which can be marked by high organic matter preservation and high metal enrichment (Tribovillard et al., 2006). The high Ni and Cu content, combined with the high V, Mo and TOC content, suggests that there were high levels of primary productivity and the water column was oxygen deficient, allowing a greater amount of organic matter to reach the seafloor and be preserved in the sediment. The TOC contents in Zone 3, for the Woodford Shale and Mississippian Limestone units, range from 9.29-9.36 wt.% and 4.8-9.09 wt.%, respectively, further supporting this interpretation. The higher amounts of TOC content in the Woodford Shale suggests that, during this time, a greater influx of terrigenous organic matter was being supplied to the sediments.

For the Woodford Shale, the pattern displayed in Figure 33 shows a progression through time from Zone 3 (anoxic-euxinic and high productivity) to Zone 1 (suboxic-anoxic and low productivity). During the time of the Woodford Shale deposition, the Late Devonian Seaway (LDS) extended across the North American craton and, due to reactivation of basement faults associated with compressional stress fields (Howell and van der Pluijm, 1990, 1999), the craton was subdivided by structural highs into a series of basins (Algeo and Tribovillard, 2009). As a consequence of these structural features, substantial bathymetric variation existed across the LDS and, thus, variable water depths existed (Algeo and Tribovillard, 2009). These bathymetric variations likely served as sills throughout the LDS, restricting deep waters in some of the basins (Algeo and Tribovillard, 2009). This reduced bottom water circulation is likely the cause for the anoxic-euxinic conditions of Zone 3 in the Woodford Shale. As time progressed, increased terrestrial weathering rates during the Late Devonian (Algeo et al., 1995, 2001; Algeo and Scheckler, 1998; Rimmer et al., 2004) provided sediment infill to the basin, allowing for enhanced organic matter preservation and a gradual increase in bottom water circulation and, later, less reducing conditions. Rimmer et al. (2004) explains that the rapid expansion of land plants throughout the Middle to Late Devonian, in terms of size and habit, is thought to have resulted in a significant increase in chemical weathering in terrestrial environments (Algeo et al., 1995, 2001; Algeo and Scheckler, 1998), and in the availability of terrestrially-derived nutrients to the oceans. This may have contributed to the high surface-water productivity that in turn resulted in excess benthic oxygen demand (Algeo et al., 1995; Rimmer et al., 2004), producing the anoxic conditions and terrigenous organic matter that we see in our Woodford Shale samples.

For the Mississippian Limestone, the pattern displayed in Figure 33 shows a kind of cyclic evolution of bottom water reducing conditions. We can see that 3 main cycles exist, each

one beginning with Zone 3 and ending with Zone 1, only to sharply jump back to Zone 3 again. During the Early to Middle Mississippian time, Oklahoma and most of the southern margin of the North American continent were covered with a wide carbonate platform (Gutschick, 1983; Al Atwah et al., 2015). Paleobathymetric settings during Mississippian time favored organic matter preservation in the carbonate rock succession (Al Atwah, 2015). Previous studies on Mississippian carbonate source rocks suggest that regional sea level events that occurred during this time allowed for the preservation of organic matter (Jiang et al., 2001; Al Atwah et al., 2015). Regional sea level events may very well be the explanation for the cyclic pattern we note in the Mississippian Limestone depositional profile. We see gradual declines in reducing conditions, as well as TOC content, from Zone 3 to Zone 1, followed by a sharp increase back to Zone 3. This may be explained by the gradual fall of sea level from Zone 3 to Zone 1, followed by a quick rise in sea level (sharp jump from Zone 1 to Zone 3). Zone 3 in the Mississippian Limestone unit allowed for organic rich layers to be deposited and preserved within the predominantly carbonate setting.

In attempting to build a schematic model for the depositional profiles for the Woodford Shale and Mississippian Limestone units, we decided to use the 3 previously discussed zones for the Woodford Shale model. However, in order to simplify the Mississippian Limestone model, we decided to group the zones into cycles, that is, each time Zone 3 progresses through time to Zone 1, one cycle has developed. If a cycle (Zone 3-Zone 1) does not fully complete (e.g. Zone 2-Zone1), this will be termed a sub-cycle. Figure 34 shows the schematic model for the Woodford Shale depositional profile and Figure 35 shows the schematic model for the Mississippian Limestone depositional profile.

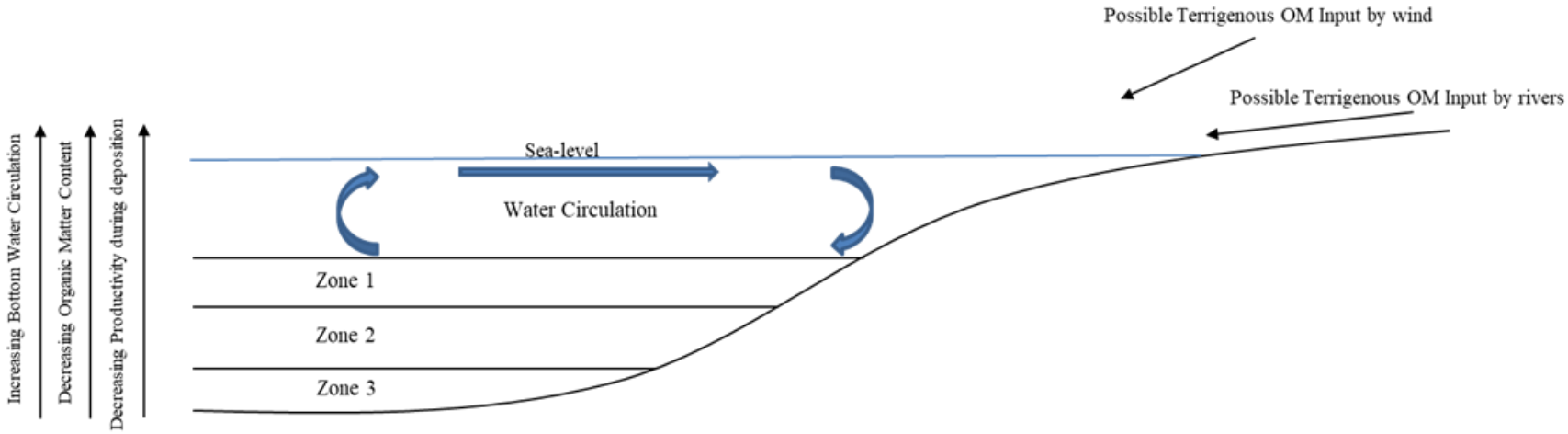

Figure 34: Schematic model of the depositional profile for the Woodford Shale. Zone 1 (suboxic-anoxic and low productivity), Zone 2 (anoxic-euxinic and low productivity) and Zone 3 (anoxic-euxinic and high productivity). Terrigenous organic matter is the predominant source.

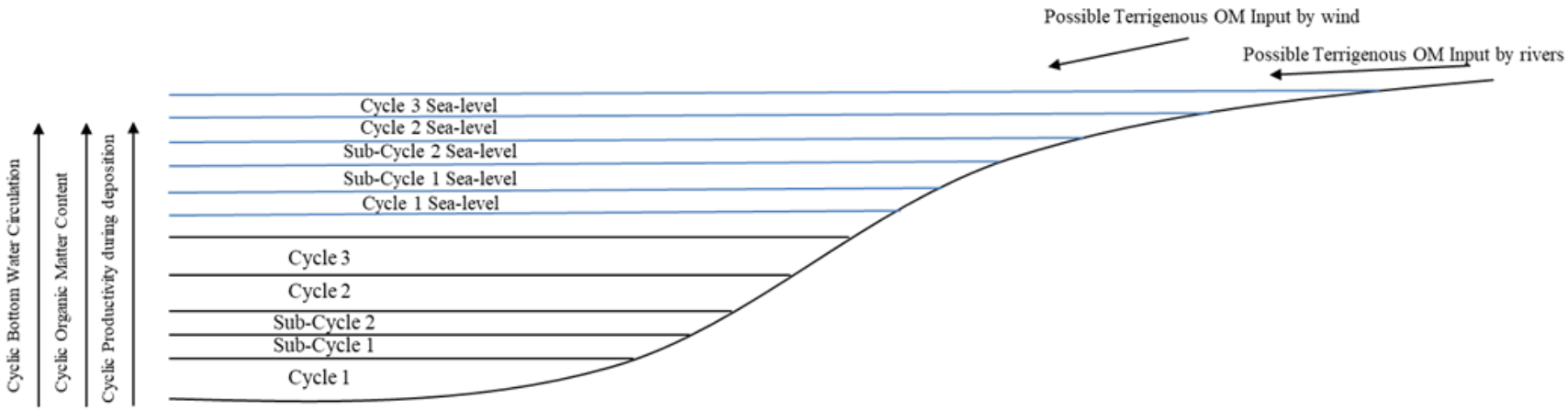

Figure 35: Schematic model of the depositional profile for the Mississippian Limestone. Each cycle consists of 3 zones: Zone 1 (suboxic-anoxic and low productivity), Zone 2 (anoxic-euxinic and low productivity) and Zone 3 (anoxic-euxinic and high productivity) and is modeled in Figure 33. Terrigenous organic matter is the predominant source.

CHAPTER VI

CONCLUSION

Using a variety of geochemical organic matter and paleoredox methodologies, we have determined that there was a predominantly terrigenous organic matter source input to the Woodford Shale and Mississippian Limestone, and the majority of the studied core samples were deposited under suboxic-anoxic conditions and low-moderate productivity, with the exception of a few samples under more reducing conditions (euxinic) and higher productivity. Schematic models of the units show that the Woodford Shale samples appear to follow a time progressive depositional profile while the Mississippian Limestone samples appear to follow a more cyclic pattern of deposition.

The oil samples were analyzed using trace element ratios to determine their organic matter origin and paleoredox conditions. Trace element ratios show that 2 of the oil samples originated from marine organic matter and a marine source rock, while 6 of the oil samples originated from terrigenous organic matter and less reducing conditions, possibly suboxic-anoxic conditions. Using these ratios, we examined oil-oil correlations, creating Group A and Group B oils, as well as oil-source rock correlations. We interpreted that the oils from Group B correlated well with the Mississippian Limestone samples. On the other hand, taking the producing location of the oils into account, we hypothesize that the oils in Group A had migrated from a location in the deep part of the basin to the shelf location at which they were produced.

The trace element ratios and enrichment factors, for the core samples and oil samples, proved to be useful in determining organic matter source and paleoredox conditions. In future

work, analyzing core and oil samples from a broader area of the basin would be optimal for better oil-oil and oil-source rock correlations.

REFERENCES

Adegoke, A.K., Abdullah, W.H., Hakimi, M.H., Yandoka, B.M.S., Mustapha, K.A. and Aturamu, A.O., 2014. Trace elements geochemistry of kerogen in Upper Cretaceous sediments, Chad (Bornu) Basin, northeastern Nigeria: Origin and paleo-redox conditions. *Journal of African Earth Sciences*, *100*, pp.675-683.

Al Atwah, I., Puckette, J., and Quan, T., 2015. Petroleum Geochemistry of the Mississippian Limestone Play, Northern Oklahoma, USA: Evidence of Two Different Charging Mechanisms East and West of the Nemaha Uplift: *AAPG Annual Convention & Exhibition, Search and Discovery Article #10773* (2015).

Al Atwah, I., Puckette, J., Pantano, J., Arouri, K. and Moldowan, J.M., 2017. Organic Geochemistry and Crude Oil Source Rock Correlation of Devonian-Mississippian Petroleum Systems in Northern Oklahoma.

Al-Shahristani, H., Al-Atyia, M., 1972. Vertical migration of oil in Iraqi oil fields: evidence based on vanadium and nickel concentrations: *Geochimica et Cosmochimica Acta, 36*(9), pp.929–938.

Algeo, T.J., and Lyons, T.W., 2006. Mo–total organic carbon covariation in modern anoxic marine environments: Implications for analysis of paleoredox and paleohydrographic conditions: *Paleoceanography, 21*(1).

Algeo, T.J., and Maynard, J.B., 2004. Trace-element behavior and redox facies in core shales of Upper Pennsylvanian Kansas-type cyclothems: *Chemical Geology, 206*, pp.289–318.

Algeo, T.J., and Maynard, J.B., 2008. Trace-metal covariation as a guide to water-mass conditions in ancient anoxic marine environments: *Geosphere, 4*(5), pp.872-887.

Algeo, T. J., and Rowe, H., 2012. Paleoceanographic applications of trace-metal concentration data: *Chemical Geology, 324*, pp.6-18.

Algeo, T.J., and Tribovillard, N., 2009. Environmental analysis of paleoceanographic systems based on molybdenum–uranium covariation: *Chemical Geology, 268*(3), pp.211-225.

Algeo, T.J., Berner, R.A., Maynard, J.B. and Scheckler, S.E., 1995. Late Devonian oceanic anoxic events and biotic crises: "rooted" in the evolution of vascular land plants: *GSA today*, *5*(3), pp.45-66.

Algeo, T.J., Scheckler, S.E. and Maynard, J.B., 2001. Effects of the Middle to Late Devonian spread of vascular land plants on weathering regimes, marine biotas, and global climate: *Plants invade the land: evolutionary and environmental perspectives*, Columbia University Press, New York, pp.213-236.

Algeo, T.J. and Scheckler, S.E., 1998. Terrestrial-marine teleconnections in the Devonian: links between the evolution of land plants, weathering processes, and marine anoxic events: *Philosophical Transactions of the Royal Society B: Biological Sciences*, *353*(1365), pp.113-130.

Akinlua, A. and Torto, N., 2011. Geochemical evaluation of Niger Delta sedimentary organic rocks: a new insight: *International Journal of Earth Sciences*, *100*(6), pp.1401-1411.

Akinlua, A., Ajayi, T.R. and Adeleke, B.B., 2007a. Organic and inorganic geochemistry of northwestern Niger Delta oils: *Geochemical journal*, *41*(4), pp.271-281.

Akinlua, A., Torto, N., Ajayi, T.R. and Oyekunle, J.A.O., 2007b. Trace metals characterization of Niger delta kerogens: *Fuel*, *86*(10-11), pp.1358-1364.

Akinlua, A., Torto, N. and Ajayi, T.R., 2008. Determination of rare earth elements in Niger Delta crude oils by inductively coupled plasma-mass spectrometry: *Fuel*, *87*(8-9), pp.1469-1477.

Akinlua, A., Adekola, S.A., Swakamisa, O., Fadipe, O.A. and Akinyemi, S.A., 2010. Trace element characterization of Cretaceous Orange Basin hydrocarbon source rocks: *Applied Geochemistry*, *25*(10), pp.1587-1595.

Akinlua, A., Sigedle, A., Buthelezi, T. and Fadipe, O.A., 2015. Trace element geochemistry of crude oils and condensates from South African Basins: *Marine and Petroleum Geology*, *59*, pp.286-293.

Akinlua, A., Olise, F.S., Akomolafe, A.O. and McCrindle, R.I., 2016. Rare earth element geochemistry of petroleum source rocks from northwestern Niger Delta: *Marine and Petroleum Geology*, *77*, pp.409-417.

Amsden, T.W., 1975. Hunton Group, Late Ordovician, Silurian, and Early Devonian in the Anadarko Basin of Oklahoma: *Oklahoma Geological Survey, University of Oklahoma*, *121*.

Amorim, F.A., Welz, B., Costa, A.C., Lepri, F.G., Vale, M.G.R. and Ferreira, S.L., 2007. Determination of vanadium in petroleum and petroleum products using atomic spectrometric techniques: *Talanta*, *72*(2), pp.349-359.

Barwise, A., 1990. Role of nickel and vanadium in petroleum classification: *Energy & Fuels*, *4*, pp.647–652.

Blakey, R., Early Mississippian (345Ma), 2017. https://www2.nau.edu/rcb7/namM345.jpg.

Blakey, R., Late Devonian (360Ma), 2017. https://www2.nau.edu/rcb7/namD360.jpg.

Boyd, D.T., 2012. Oklahoma 2011 Drilling Highlights.

Brumsack, H.J., 1989. Geochemistry of recent TOC-rich sediments from the Gulf of California and the Black Sea: *Geologische Rundschau, 78*(3), pp.851-882.

Brumsack, H.J., 2006. The trace metal content of recent organic carbon-rich sediments: implications for Cretaceous black shale formation: *Paleogeography, Paleoclimatology, Paleoecology, 232*(2), pp.344-361.

Burchett, R.R., 1983. Surface to subsurface correlation of Pennsylvanian and lower Permian rocks across southern Nebraska: *Conservation and Survey Division, University of Nebraska*, (8).

Calvert, S.E., Pedersen, T.F., 1993. Geochemistry of Recent oxic and anoxic marine sediments: Implications for the geological record: *Marine Geology, 113*, pp.67–88.

Cardott, B.J. and Lambert, M.W., 1985. Thermal maturation by vitrinite reflectance of Woodford Shale, Anadarko basin, Oklahoma: *AAPG Bulletin, 69*(11), pp.1982-1998.

Carlson, M.P., 1971. Eastern Nebraska and north-central Kansas; in, Future Petroleum Provinces of the United States-Their Geology and Potential: *American Association of Petroleum Geologists Memoir, 15*, pp.1-103.

Cronenwett, C.E., 1956, A subsurface study of the Simpson Group in east-central Oklahoma: Oklahoma City Geological Society: *Shale Shaker Digest*, (2), pp.171-187.

Curiale, J.A., 1987. Distribution of transition metals in North Alaska oils: Metal complexes in fossil fuels: *ACS Symposium Series, 344*, pp.135–145.

Denison, R.E., Lidiak, E.G., Bickford, M.E., and Kisvarsanyi, E.B., 1984. Geology and geochronology of Precambrian rocks in the central interior region of the United States: *U.S. Geological Survey Professional Paper, 1241*(C), pp.1-20.

Dolton G.L., Finn, T.M., 1989. Petroleum Geology of the Nemaha Uplift, Central Midcontinent: *U.S. Geological Survey Open-File Report, 88*(450D), pp.1-18.

Donovan, R.N., Beachamp, W., Ferraro, T., Lajek, D., McConnell, D., Munsil, M., Ragland, D., Sweet, B., and Taylor, D., 1983. Subsidence rates in Oklahoma during the Paleozoic: *Oklahoma City Geological Society, Shale Shaker, 33*, pp.86-88.

Ellrich, J., Hirner, A., Stark, H., 1985. Distribution of trace elements in crude oils from southern Germany: *Chemical Geology, 48*, pp.313–323.

Emerson, S.R., Huested, S.S., 1991. Ocean anoxia and the concentration of molybdenum and vanadium in seawater: *Marine Chemistry, 34*, pp.177–196.

Filby, R.H., 1994. Origin and nature of trace elements species in crude oils, bitumens and kerogens: implications for correlation and other geochemical studies: *Geological Society, London, Special Publication, 78*(1), pp.203–219.

Franseen, E.K., 2006. Mississippian (Osagean) shallow-water, mid-latitude siliceous sponge spicule and heterozoan carbonate facies: An example from Kansas with implications for regional controls and distribution of potential reservoir facies: *Kansas Geological Survey*.

Frezon, S.E. and Jordan, L., 1979. Paleotectonic Investigations of the Mississippian System in the United States, Part I: Introduction and Regional Analyses of the Mississippian System: *Paleotectonic investigations of the Mississippian System in the United States*, (1010), pp.145.

Fu, X., Wang, J., Zeng, Y., Cheng, J., Tano, F., 2011. Origin and mode of occurrence of trace elements in marine oil shale from the Shengli River Area, Northern Tibet, China: *Oil Shale, 28*, pp.487–506.

Galarraga, F., Reategui, K., Martïnez, A., Martínez, M., Llamas, J.F. and Márquez, G., 2008. V/Ni ratio as a parameter in palaeoenvironmental characterization of nonmature medium-crude oils from several Latin American basins: *Journal of Petroleum Science and Engineering*, *6*(1), pp.9-14.

Gao, P., Liu, G., Jia, C., Ding, X., Chen, Z., Dong, Y., Zhao, X. and Jiao, W., 2015. Evaluating rare earth elements as a proxy for oil–source correlation: A case study from Aer Sag, Erlian Basin, northern China: *Organic Geochemistry, 87*, pp.35-54.

Glikson, M., Chappell, B.W., Freeman, R.S. and Webber, E., 1985. Trace elements in oil shales, their source and organic association with particular reference to Australian deposits: *Chemical Geology, 53*(1-2), pp.155-174.

Greibrokk, T., Lundanes, E., Norli, H.R., Dyrstad, K., Olsen, S.D., 1994. Experimental simulation of oil migration-distribution effects on organic compound groups and on metal/metal ratios: *Chemical Geology, 116*, pp.281–299.

Gutschick, R.C., and Sandberg, C.A., 1983. Mississippian Continental Margins of the Conterminous Unites States, in Stanley, D.J., and Moore, G.T., The Shelfbreak: Critical Interface on Continental Margins: *Society of Economic Paleontologists and Mineralogists, Special Publication*, (33), pp.79-96.

Hair, T.J., 2012. Constructing a geomechanical model of the Woodford Shale, Cherokee Platform, Oklahoma, USA effects of confining stress and rock strength on fluid flow: *Doctoral dissertation, Texas Christian University*.

Harris, N.B., Freeman, K.H., Pancost, R.D., White, T.S., Mitchell, G.D., 2004. The character and origin of lacustrine source rocks in the Lower Cretaceous synrift section, Congo Basin, West Africa: *AAPG Bulletin, 88*, pp.1163–1184.

Hatch, J.R., Leventhal, J.S., 1992. Relationship between inferred redox potential of the depositional environment and geochemistry of the Upper Pennsylvanian (Missourian)

stark shale member of the Dennis Limestone, Wabaunsee County, Kansas, USA: *Chemical Geology, 99*, pp.65-82.

Hirner, A.V., 1987. Metals in crude oils, asphaltenes, bitumen, and kerogen in Molasse Basin, Southern Germany: *Metal Complexes in Fossil Fuels, 344, ACS Symposium Series*, pp.146–153.

Hirner, A.V. and Xu, Z., 1991. Trace metal speciation in Julia Creek oil shale: *Chemical Geology, 91*(2), pp.115-124.

Hitchon, B., Filby, R.H., 1984. Use of trace elements for classification of crude oils into families—examples for Alberta, Canada: *AAPG Bulletin, 68*, pp.838–849.

Howell, P.D., van der Pluijm, B.A., 1990. Early history of the Michigan Basin: subsidence and Appalachian tectonics: *Geology, 18*, pp.1195–1198.

Howell, P.D., van der Pluijm, B.A., 1999. Structural sequences and styles of subsidence in the Michigan Basin: *GSA Bulletin, 111*, pp.974–991.

Jiao, W., Yang, H., Zhao, Y., Zhang, H., Zhou, Y., Zhang, J., Xie, Q., 2010. Application of trace elements in the study of oil–source correlation and hydrocarbon migration in the Tarim Basin, China: *Energy, Exploration & Exploitation, 28*, pp.451–466.

Jiang, C., Li, M., Osadetz, K.G., Snowdon, L.R., Obermajer, M. and Fowler, M.G., 2001. Bakken/Madison petroleum systems in the Canadian Williston Basin, Part 2: molecular markers diagnostic of Bakken and Lodgepole source rocks: *Organic Geochemistry, 32*(9), pp.1037-1054.

Jin, Q., Tian, H.Q. and Dai, J.S., 2001. Application of microelement composition to the correlation of solid bitumen with source rocks: *Petroleum Geology and Experiment, 23*(3), pp.285-290.

Johnson, J.G., Sandberg, C.A. and Poole, F.G., 1988. Early and Middle Devonian paleogeography of western United States: *Devonian of the World: Proceedings of the 2nd International Symposium on the Devonian System, 14*(1), pp.161-182

Johnson, K.S., Amsden, T.W., Denison, R.E., Goldstein, A.G., Dutton, S.P., Rascoe, J.B., Sutherland, P.K., and Thompson, C.M., 1989. Geology of the Southern Midcontinent: *Oklahoma Geological Survey Special Publication, 89*(2), pp.1-53.

Jones, B., Manning, D.A.C., 1994. Comparison of geochemical indices used for the interpretation of paleoredox conditions in ancient mudstone: *Chemical Geology, 111*, pp.111–129.

Kelly, C., 2016. Potential Volcanic Ash Fertilization of the Western Interior Seaway, Cenomanian-Turonian: ICP-MS Analysis of the Eagle Ford Formation: *Masters Thesis, Texas A&M University*.

Klemme, H., and Ulmishek, G. F., 1991. Effective petroleum source rocks of the world: stratigraphic distribution and controlling depositional factors: *AAPG Bulletin, 75*(12), pp.1809-1851.

Koch, J.T., Frank, T.D. and Bulling, T.P., 2014. Stable-isotope chemostratigraphy as a tool to correlate complex Mississippian marine carbonate facies of the Anadarko shelf, Oklahoma and Kansas: *AAPG Bulletin, 98*(6), pp.1071-1090.

Lane, H.R. and De Keyser, T.L., 1980. Paleogeography of the late Early Mississippian (Tournaisian 3) in the central and southwestern United States: *Rocky Mountain Section (SEPM)*.

Lewan, M.D., 1980. Geochemistry of vanadium and nickel in organic matter of sedimentary rocks: *Ph.D. Dissertation, University of Cincinnati*.

Lewan, M.D., 1984. Factors controlling the proportionality of vanadium and nickel in crude oils: *Geochimica et Cosmochimica Acta, 48,* pp.2231–2238.

Lewan, M.D., Maynard, J.B., 1982. Factors controlling enrichment of vanadium and nickel in the bitumen of organic sedimentary rocks: *Geochimica et Cosmochimica Acta, 46*, pp.2547–2560.

Little, S.H., Vance, D., Lyons, T.W. and McManus, J., 2015. Controls on trace metal authigenic enrichment in reducing sediments: insights from modern oxygen-deficient settings: *American Journal of Science, 315*(2), pp.77-119.

Lo Mónaco, S., López, L., Rojas, H., Garcia, D., Premovic, P. and Briceño, H., 2002. Distribution of major and trace elements in La Luna Formation, southwestern Venezuelan basin: *Organic geochemistry, 33*(12), pp.1593-1608.

López, L., Lo Mónaco, S., Galarraga, F., Lira, A., and Cruz, C., 1995. V/Ni ratio in maltene and asphaltene fractions of crude oils from the west Venezuelan Basin: correlation studies: *Chemical Geology, 119*, pp.255–262.

López, L. and Lo Mónaco, S., 2017. Vanadium, nickel and sulfur in crude oils and source rocks and their relationship with biomarkers: Implications for the origin of crude oils in Venezuelan basins: *Organic geochemistry, 104*, pp.53-68.

Lowe, D.R., 1975. Regional controls on silica sedimentation in the Ouachita system: *GSA Bulletin, 86*(8), pp.1123-1127.

Lyons, T.W., Werne, J.P., Hollander, D.J., and Murray, R.W., 2003. Contrasting sulfur geochemistry and Fe/Al and Mo/Al ratios across the last oxic-to-anoxic transition in the Cariaco Basin, Venezuela: *Chemical Geology, 195*, pp.131–157.

MacDonald, R., Hardman, D., Sprague, R., Meridji, Y., Mudjiono, W., Galford, J., Rourke, M., Dix, M., and Kelto, M., 2010. Using elemental geochemistry to improve sandstone

reservoir characterization: a case study from the Unayzah A interval of Saudi Arabia: *SPWLA 51st Annual Logging Symposium*, pp.1–16.

Mazzullo, S.J., Wilhite, B.W. and Woolsey, I.W., 2009. Petroleum reservoirs within a spiculite-dominated depositional sequence: Cowley Formation (Mississippian: Lower Carboniferous), south-central Kansas: *AAPG bulletin*, *93*(12), pp.1649-1689.

McBee, W., 2003. The Nemaha and Nearby Fault Zones in the Context of Midcontinent Strike-Slip Structural Geology: *Abstracts-AAPG Mid-Continent Section Meeting*.

McLennan, S.M., 2001. Relationships between the trace element composition of sedimentary rocks and upper continental crust: *Geochemistry, Geophysics, Geosystems, G3*(2), (paper # 2000GC000109).

McManus, J., Berelson, W.M., Hammond, D.E., Klinkhammer, G.P., 1999. Barium cycling in the North Pacific: implication for the utility of Ba as a paleoproductivity and paleoalkalinity proxy: *Paleoceanography, 14*, pp.62–73.

Montgomery, S.L., Mullarkey, J.C., Longman, M.W., Colleary, W.M. and Rogers, J.P., 1998. Mississippian chat reservoirs, south Kansas: Low-resistivity pay in a complex chert reservoir: *AAPG bulletin*, *82*(2), pp.187-205.

Morford, J.L. and Emerson, S., 1999. The geochemistry of redox sensitive trace metals in sediments: *Geochimica Cosmochimica Acta, 63*, pp.1735–1750.

Morford, J., Russell, A., and Emerson, S., 2001. Trace metal evidence for changes in the redox environment associated with the transition from terrigenous clay to diatomaceous sediment, Saanich Inlet, BC: *Marine Geology, 174*(1), pp.355-369.

Mudiaga, O.C., Nicolas, O.C. and Leo, O.C., 2011. Trace metals geochemistry of crude oils from Umutu/Bomu fields in south west Niger delta Nigeria: *Energy and Environment Research*, *1*(1), pp.139.

Northcutt, R. A., Johnson, K. S., and Hinshaw, G. C., 2001. Geology and Petroleum Reservoirs in Silurian, Devonian, and Mississippian Rocks in Oklahoma: *Oklahoma Geological Survey, Silurian, Devonian, and Mississippian Geology and Petroleum in the Southern Midcontinent, 1999 Symposium, Circular 105*, pp.1-15.

Nwachukwu, J.I., Oluwole, A.F., Asubiojo, O.I., Filby, R.H., Grimm, C., and Fitzgerald, S.A., 1995. Geochemical evaluation of Niger Delta crude oils: *Geology of deltas*, pp.287–300.

Oluwole, A.F., Asubiojo, O.I., Nwachukwu, J.I., Ojo, J.O., Ogunsola, O.J., Adejumo, J.A., Filby, R.H., Fitzgerald, S. and Grimm, C., 1993. Neutron activation analysis of Nigerian crude oils: *Journal of radioanalytical and nuclear chemistry, 168*(1), pp.145-152.

Peters, K.E. and Moldowan, J.M., 1993. The biomarker guide: interpreting molecular fossils in petroleum and ancient sediments. United States.

Piper, D.Z., Perkins, R.B., 2004. A modern vs. Permian shale - the hydrography, primary productivity, and water-column chemistry of deposition: *Chemical Geology, 206*, pp.177–197.

Piper, D.Z., Perkins, R.B., Rowe, H.D., 2007. Rare-earth elements in the Permian Phosphoria Formation: paleo proxies of ocean geochemistry: *Deep-Sea Research II, 54*, pp.1396–1413

Qi, H., Hu, R. and Zhang, Q., 2007. Concentration and distribution of trace elements in lignite from the Shengli Coalfield, Inner Mongolia, China: Implications on origin of the associated Wulantuga Germanium Deposit: *International Journal of Coal Geology, 71*(2-3), pp.129-152.

Rimmer, S.M., 2004. Geochemical paleoredox indicators in Devonian–Mississippian black shales, Central Appalachian Basin (USA): *Chemical Geology, 206*, pp.373–391.

Rimmer, S.M., Thompson, J.A., Goodnight, S.A., and Robl, T.L., 2004. Multiple controls on the preservation of organic matter in Devonian–Mississippian marine black shales: geochemical and petrographic evidence: *Paleogeography, Paleoclimatology, Paleoecology, 215*, pp.125–154.

Rogers, S.M., 2001. Deposition and diagenesis of Mississippian chat reservoirs, north-central Oklahoma: *AAPG bulletin, 85*(1), pp.115-129.

Shaw, T.J., Gieskes, J.M., and Jahnke, R.J., 1990. Early diagenesis in differing depositional environments: the response of transition metals in porewater: *Geochimica Cosmochimica Acta, 54*, pp.1233–1246.

Shi, C., Cao, J., Bao, J., Zhu, C., Jiang, X., and Wu, M., 2015. Source characterization of highly mature pyrobitumens using trace and rare earth element geochemistry: Sinian-Paleozoic paleo-oil reservoirs in south China: *Organic Geochemistry, 83*, pp.77–93.

Stow, D.A.V. and Atkin, B.P., 1987. Sediment facies and geochemistry of Upper Jurassic mudrocks in the central North Sea area: *Petroleum Geology of North West Europe*, pp.797-808.

Taylor, S.R., and McLennan, S.M., 1985. The Continental Crust: Its Composition and Evolution: Blackwell, Oxford, UK, pp.312.

Tissot, B.P., and Welte, D.H., 1984. Petroleum Formation and Occurrence, 2nd ed. Springer-Verlag, Berlin, Heidelberg, New York, Tokyo, pp.408–497.

Tribovillard, N., Algeo, T. J., Lyons, T., and Riboulleau, A., 2006. Trace metals as paleoredox and paleoproductivity proxies: an update: *Chemical geology, 232*(1), pp.12-32.

Tribovillard, N., Bout-Roumazeilles, V., Algeo, T., Lyons, T.W., Sionneau, T., Montero-Serrano, J.C., Riboulleau, A., and Baudin, F., 2008. Paleodepositional conditions in the

Orca Basin as inferred from organic matter and trace metal contents: *Marine Geology, 254*, pp.62–72.

Tyson, R., and Pearson, T., 1991. Modern and ancient continental shelf anoxia: an overview: *Geological Society, London, Special Publications, 58*(1), pp.1-24.

Udo, O.T., Ekwere, S., and Abrakasa, S., 1992. Some trace metals in selected Niger Delta crude oils: application in oil–oil correlation studies: *Journal of Mineralogy Geology, 28,* pp.289–291.

Van der Weijden, C.H., 2002. Pitfalls of normalization of marine geochemical data using a common divisor: *Marine Geology, 184*(3), pp.167-187.

Watney, W.L., Guy, W.J. and Byrnes, A.P., 2001. Characterization of the Mississippian chat in south-central Kansas: *AAPG Bulletin, 85*(1), pp.85-113.

Watney, W.L., Franseen, E.K., Byrnes, A.P. and Nissen, S.E., 2008. Contrasting styles and common controls on Middle Mississippian and Upper Pennsylvanian carbonate Platforms in the Northern Midcontinent, USA, Controls on Carbonate Platform and Reef Development: *SEPM Special Publication, 89*, pp.125-145.

Wedepohl, K.H., 1971. Environmental influences on the chemical composition of shales and clays: *Physics and Chemistry of the Earth, 8*, Pergamon, Oxford (1971), pp.305–333.

Wedepohl, K.H., 1991. The composition of the upper earth's crust and the natural cycles of selected metals, Metals in natural raw materials, Natural Resources: *Metals and Their Compounds in the Environment*, VCH, Weinheim, pp.3–17.

Witzke, B.J., 1990. Paleoclimatic constraints for Paleozoic paleolatitudes of Laurentia and Euramerica: *Geological Society, London, Memoirs, 12*(1), pp.57-73.

Zhao, Y., Liu, C.Y., Niu, H.Q., Zhao, X.C., Zhang, D.D., Yang, D. and Deng, H., 2017. Trace and rare earth element geochemistry of crude oils and their coexisting water from the Jiyuan Area of the Ordos Basin, N China: *Geological Journal, 53*(1), pp.336-348.

Ziegler, P.A., 1989, Discussion: Evolution of Laurussia, pp.67-76.

APPENDIX A

Table 7: Trace element concentrations for the core sample set using Rock Eval pyrolysis method (n.d. means not determined).

Interval	Sample	Depth	TOC	Ti	Mn	Ni	Cu	U	Na	Mg	Al	S	Cr	Fe	K
		ft.	wt. %	ppm	ppm	ppm	ppm	ppm	ppm	ppm	ppm	ppm	ppm	ppm	ppm
Mississippian Limestone	1	4,968.5	2.2	2,120	196	83	30	1	6,064	531	30,639	5,035	348	15,556	11,892
	2	4,972	2.1	4,151	150	282	38	N.d.	10,060	949	72,623	3,207	361	24,387	28,261
	3	4,973	1.7	3,352	201	124	29	1	7,668	882	59,283	7,203	345	24,238	22,795
	4	4,975	4.0	2,452	178	420	39	N.d.	6,525	622	33,161	7,015	488	20,966	14,310
	5	4,983	9.1	2,762	126	221	45	9	7,025	627	40,237	3,507	407	14,752	14,416
	6	4,992	4.4	2,757	161	161	40	10	8,376	819	44,173	4,630	394	19,746	18,123
	7	5,022	1.8	2,837	124	125	26	1	9,752	617	34,663	1,859	227	10,075	12,635
	8	5,033	2.7	2,934	277	107	37	N.d.	8,370	1202	42,237	5,136	196	21,835	16,609
	9	5,044	4.0	1,618	159	161	26	21	6,754	785	34,527	4,309	257	15,932	12,225
	10	5,050	6.9	3,191	118	269	56	5	7,823	778	51,392	4,599	388	18,639	20,245
	11	5,055	2.7	3,559	129	133	35	5	8,998	789	52,703	3,978	287	17,980	19,829
	12	5,059	2.8	4,446	127	585	53	N.d.	11,236	914	67,224	259	576	26,086	25,992
	13	5,075	5.0	2,686	137	150	31	16	7,480	803	41,301	5,033	287	14,322	15,692
	14	5,086	1.8	3,272	128	156	28	N.d.	8,215	842	47,476	3,802	199	17,494	19,226
	15	5,091	1.9	3,780	150	406	54	2	10,260	935	56,350	4,482	214	21,357	21,469
	16	5,099	1.3	3,252	191	149	25	N.d.	8,768	1123	42,981	4,159	207	19,957	18,090
	17	5,108	2.2	2,608	142	203	21	3	5,893	762	33,774	5,212	288	14,169	13,244
	18	5,112	3.6	2,531	119	151	28	1	6,144	805	40,894	3,893	212	14,264	16,808
	19	5,117	2.4	5,127	270	427	63	5	11,086	12734	67,363	5,400	318	23,735	35,201
	20	5,120	3.1	5,589	466	668	64	6	12,513	13205	79,766	5,823	369	28,710	24,159
	21	5,147	0.5	3,127	311	117	17	3	6,973	15134	37,144	6,065	180	17,404	8,281
	22	5,150	0.6	2,451	529	75	8	2	5,825	27304	28,529	7,246	131	19,164	16,340
	23	5,156	4.4	5,157	290	836	77	7	11,301	13628	74,233	6,020	381	28,962	36,255
	24	5,160	2.7	4,188	432	319	46	5	8,957	12176	60,803	9,729	229	26,473	18,029
	25	5,171	5.5	6,486	261	477	63	26	12,856	11271	74,947	8,830	708	28,150	22,727
	26	5,184	4.8	3,242	244	417	42	22	6,392	8491	38,975	6,719	730	14,011	11,599
	27	5,195	2.8	4,622	461	144	37	6	10,347	14316	55,043	9,082	229	21,973	24,164
Woodford Shale	28	5,201	5.9	4,363	296	880	121	12	6,832	12382	90,315	3,901	1849	37,997	44,108
	29	5,210	2.1	3,322	433	176	62	6	5,334	14231	71,082	7,471	141	24,129	28,382
	30	5,224	5.8	2,870	301	344	56	33	4,386	12712	59,784	4,311	553	21,108	23,201
	31	5,248	9.0	3,298	636	408	91	29	6,009	18478	69,424	10,152	198	40,289	32,728
	32	5,253	9.3	2,611	266	406	83	63	4,906	9747	51,750	6,933	258	70,924	15,556
	33	5,262	9.4	2,833	436	312	81	57	6,492	15530	55,338	10,043	60	71,862	22,565